ADVANCED SIMULATION OF AN OPERATING ROOM: FROM THE VIRTUAL MODEL TO THE DIGITAL TWIN

PhD in Design, Manufacturing and Operations Engineering XXXV – A.Y. 2021/22

Tutor: Prof. M.E. Biancolini

Supervisor: Dr. M. Grigioni

Candidate: Giovanna Gargiulo

Outline

- ➢ Digital Twin: where and why
- ➢ Digital Twin & CFD and workflow
- ➢ Mathematical models
- ➢ The ventilation systems in operating theatre: requirements and configurations
- ➢ Software & tools
- ➢ Case study: the S. Gerardo operating theatre
  - The geometrical model
  - The CFD Setup
  - Operating theatre model with cylindrical dummy
  - Operating theatre model with human dummy
  - Operating theatre model with human dummy & CO_2
  - ROM setup
  - Design of Experiment
  - ROM vs ROM
  - CFD vs ROM
  - Twin Builder – Digital Twin
  - Subscale model
- ➢ Beyond S. Gerardo’s simplified model
  - Complete model: lamp positions and size effects
  - Complete model: different ventilation systems
- ➢ Conclusions

Digital Twin: where use it?

The research goal is the build of an operating theater Digital Twin (**DT**).

Definitions of **DT** are:
megamodel, device shadow, mirrored system, avatar, or synchronized virtual prototype

The main areas of interest for a **DT**:

- Meteorology
- Manufacturing and process technology
- Education
- Cities, transportation, and energy sector
- Health

In Air Quality control a **DT** can be an essential help in:

- operating room
- offices
- waiting rooms
- common areas

by providing technology for air quality control, energy saving in buildings, regulation and management of people flow, maintenance, detection, and management of plant failures.

Digital Twin: why use it?

The advantages to employ a DT could be:

Design and optimization	→	Operations and management of systems in the mechanical, thermal, electronic fields
Maintenance	→	Determination of the most stressed elements, possible replacement, identification of anomalies
Control and setting of systems	→	Improvement of efficiency, minimization of malfunction risks
IIoT interfaces	→	Definition of the elements to be modeled and transmission of the actions to be performed via device: the integration takes place via physical and virtual sensors

⇨ **Cost reduction**

Toward the digital twin: the workflow

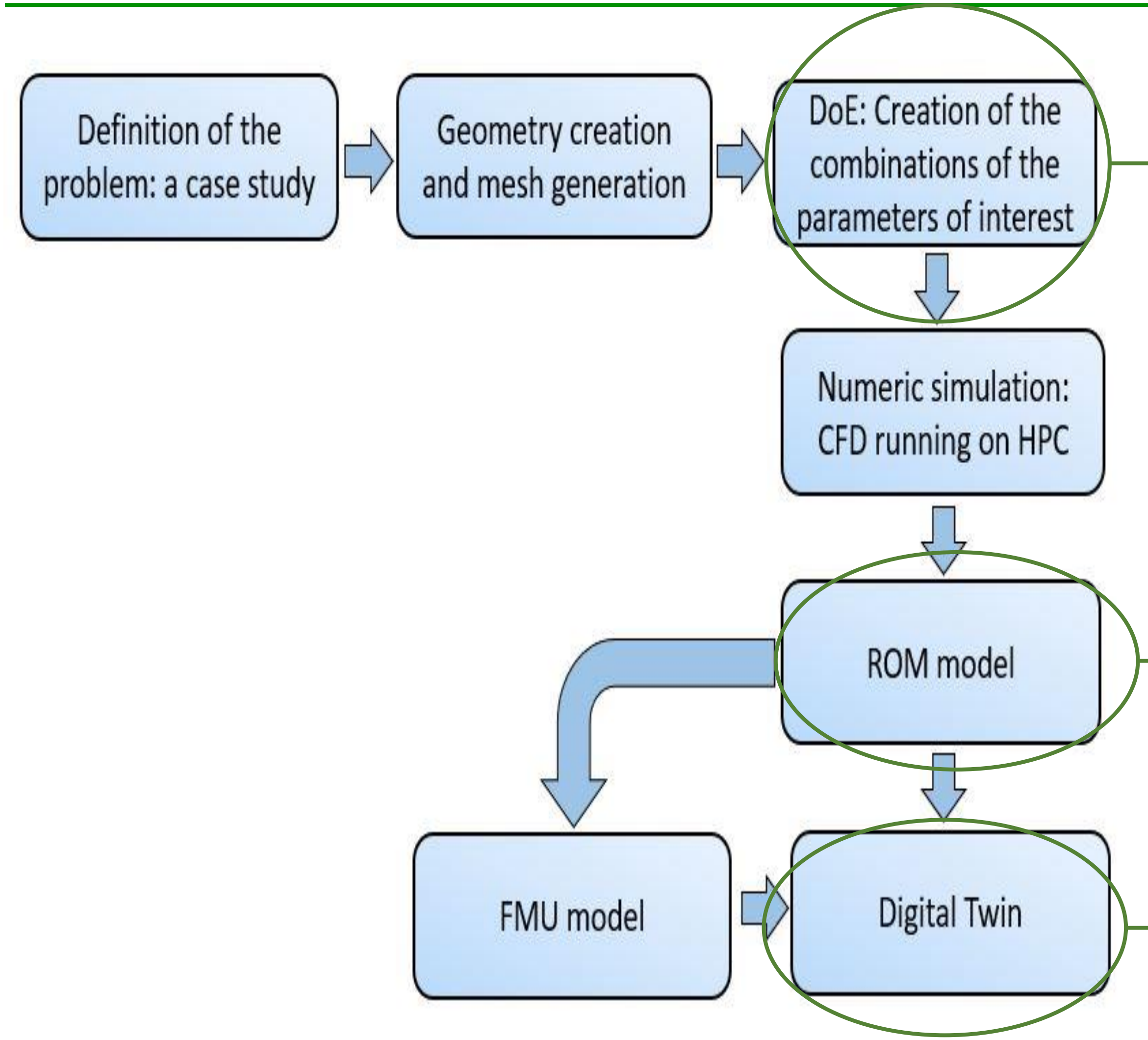

The definition of :

- set of parameters
- range of interest of parameters
- parameter combinations to give to CFD

The definition of :

- CFD set of snapshots and splitting in two sets:
  - learning set
  - validation set
- creation of Reduced Order Model by
  - SVD (Singular Value Decomposition)
  - GARS (Genetic Aggregation Response Surface)

Model export to obtain the Digital Twin (DT)

Digital Twin & CFD

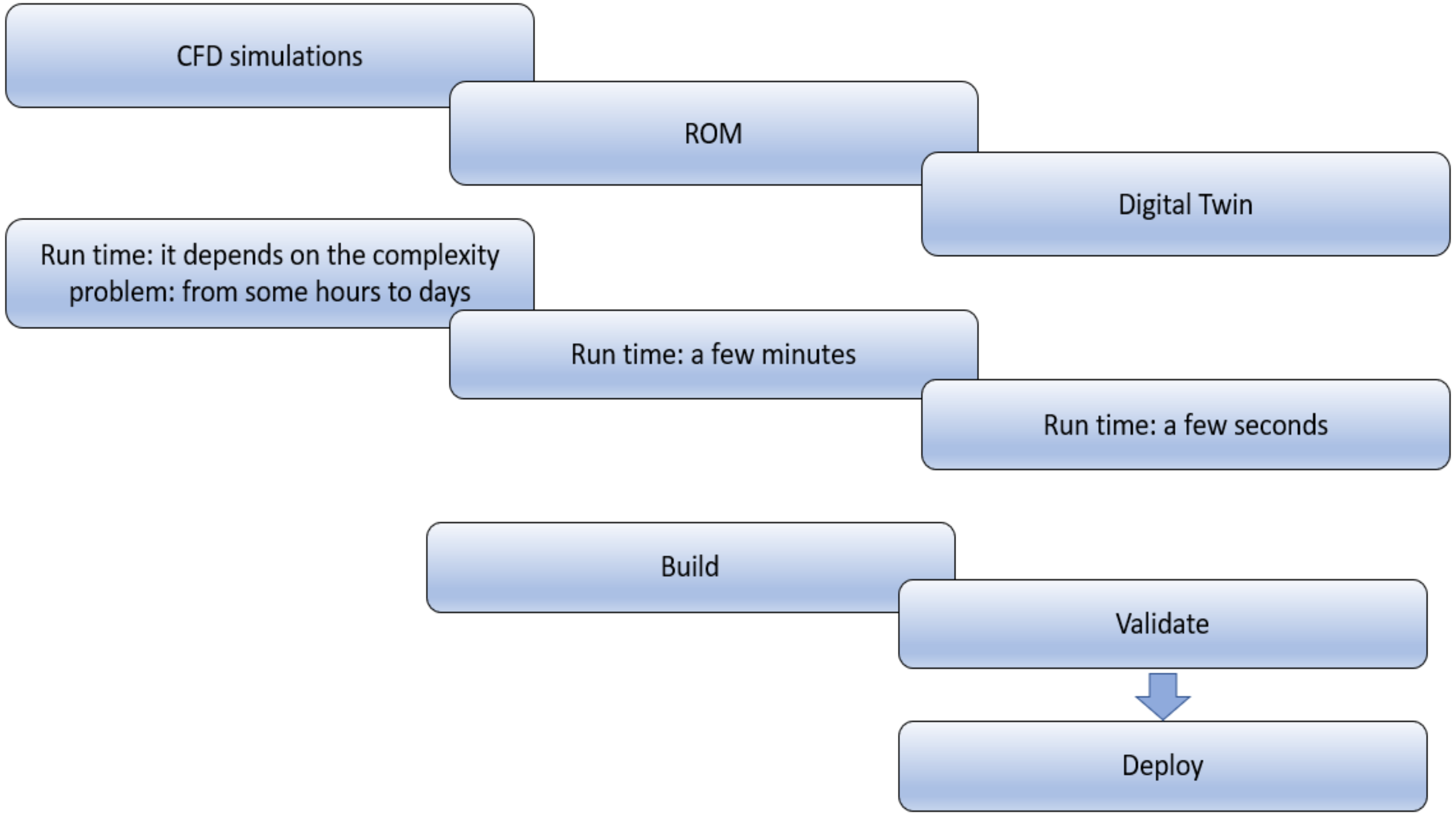

The advantages of DT with respect to CFD:

- the capability of DT to obtain the results in every point of parameter field used to created it, in few seconds after the construction
- the possibility to deploy the DT and use it on IIoT interface or a device

Mathematical Model: CFD Governing Equations

Incompressible ideal gas law, continuity, momentum, and energy equations and conservation of species in mixture model with the add the vapor H_2O to the air

$$\rho = \frac{P}{\frac{R}{M_w} T}$$

$$\frac{\partial \rho}{\partial t} + \nabla \cdot (\rho \mathbf{v}) = S_m$$

$$\frac{\partial (\rho \mathbf{v})}{\partial t} + \nabla \cdot (\rho \mathbf{v}\mathbf{v}) = -\nabla p + \nabla \cdot (\bar{\bar{\boldsymbol{\tau}}}) + \rho \mathbf{g} + \mathbf{F}$$

with $\bar{\bar{\boldsymbol{\tau}}}$ the tensor stress $\quad \bar{\bar{\boldsymbol{\tau}}} = \mu\left(\left(\nabla \mathbf{v} + \nabla \mathbf{v}^T\right)\right) - \frac{2}{3} \nabla \cdot \mathbf{v}\, \mathbf{I}$

$$\frac{\partial (\rho \mathbf{E})}{\partial t} + \nabla \cdot \left(\mathbf{v}(\rho E + p)\right) = \nabla \cdot (k_{eff} \nabla T) + S_h$$

$$\frac{\partial \rho \phi_k}{\partial t} + \frac{\partial}{\partial x_i}\left(\rho u_i \phi_k - \Gamma_k \frac{\phi_k}{\partial x_i}\right) = S_{\phi_k} \qquad k= 1, \ldots, N$$

The integral form of governing equation using the pseudo time method for a steady-state case

$$\int_V \frac{\partial (\rho \boldsymbol{\Phi})}{\partial \tau} dV + \oint_S (\rho \boldsymbol{\Phi} \mathbf{v})\, dA = \oint_S \Gamma_\Phi (\nabla \boldsymbol{\Phi})\, dA + \int_V S_\Phi\, dV$$

The pseudo time step size that can be computed using the local or global time step method

$$\rho_p \Delta V \frac{\Phi_p - \Phi_p^{old}}{\Delta \tau} + a_p \Phi_p = \sum_{nb} a_{nb} \Phi_{nb} + b$$

Φ_p^{old} is the value of Φ_p at the previous iteration and $\Delta\tau$ is the pseudo time step

Mathematical Model: Radial Basis Functions (RBF)

$$s(\mathbf{x}) = \sum_{i=1}^{N} \gamma_i \varphi\left(\|\mathbf{x} - \mathbf{x}_{ki}\|\right) + h(\mathbf{x})$$

$$\sum_{i=1}^{N} \gamma_i\, h(\mathbf{x}_{ki}) = 0 \qquad s(\mathbf{x}_{ki}) = g_i\,, \qquad 1 \le i \le N$$

$$h(\mathbf{x}) = \beta_1 + \beta_2 x + \beta_3 y + \beta_4 z$$

$$s_x(\mathbf{x}) = \sum_{i=1}^{N} \gamma_i^x\ \varphi\ (\mathbf{x} - \mathbf{x}_{ki}) + \beta_1^x + \beta_2^x x + \beta_3^x y + \beta_4^x z$$

$$s_y(\mathbf{x}) = \sum_{i=1}^{N} \gamma_i^y\ \varphi\ (\mathbf{x} - \mathbf{x}_{ki}) + \beta_1^y + \beta_2^y x + \beta_3^y y + \beta_4^y z$$

$$s_z(\mathbf{x}) = \sum_{i=1}^{N} \gamma_i^z\ \varphi\ (\mathbf{x} - \mathbf{x}_{ki}) + \beta_1^z + \beta_2^z x + \beta_3^z y + \beta_4^z z$$

Scalar function s(x) is

- a transformation $\mathbb{R}^n \rightarrow \mathbb{R}$
- defined for each arbitrary point in space x

The movement of a point can be considered as the Euclidean distance between source x_{ki} and target points x multiplied by the radial function ϕ and the weight γ_i.

The minimum degree of the **polynomial h(x)** depends on the choice of the basis function

The **desired function values g_i** are obtained at source points

The **interpolation** of a **3D set** of **displacement at source points**

Mathematical model: Reduced Order Model (ROM)

$$\mathbf{A} = \mathbf{P}\Delta\mathbf{Q}^{\mathrm{T}}$$

The **SVD** considers a **rectangular matrix (A)** decomposed into:

- two **orthogonal** matrices (**P, Q**)
- one **diagonal** matrix (**Δ**)

$$\mathrm{v}(\mathbf{x}) = \sum_{\mathrm{i}=1}^{\mathrm{r}} \mathrm{GARS}_{\mathrm{i}}(\mathbf{x})\ \mathrm{mode}_{\mathrm{i}}\,(\mathbf{x})$$

Each dataset is **linearly expressed with a set of scalar coefficients** by **using** a genetic aggregation response surface (**GARS**) technique, Ben Salem [17]
The **variable v** is the **aggregation** of **the product of the response surface** factor **and** the **mode** data for **all of the modes r**

- The **number** of **singular values r** gives the **tolerance error**
- The **modes** give the **result of the approximation**

The ROM construction implies the split of snapshots into two sets:

- **learning set** to build a **basis of modes** used **to express each solution as** a **linear combination of the modes**
- **validation** set

In addition are definite:

the curve **Reduction** represents the precision of the learning set with respect to the number of modes

the curve **LOO (Leave One Out) defines** the **precision of the base** of the modes for **a snapshot not included** in **the learning set**

Ventilation systems requirements: operating room

- **Ventilation system**: VCCC (Contamination Controlled Ventilation and Conditioning System):
- regulatory framework **ISO14644** – **UNI 11425:2011**
- VCCC system characteristics (**ISO 14644**):
- **Number of changes** with external air at least 15/h
- **Room sizes**:
- 30 m^2 and 90 m^3 -> 1350 m^3 /h
- Air filtration: HEPA filters (High Efficiency Particulate Air) 99.97%

- **Microbial contamination values**:
- 20 CFU/ m^3 in ambient air
- 1 CFU/ m^3 in the air introduced by the plant
- 0.5 CFU/ cm^2 on wall surfaces
- 0.5 CFU/ cm^2 on worktop surfaces
- **Colony forming units (CFU) ≤ 1 CFU/ m^3**

- **Operating Room**: surfaces between 25 and 36 m^2 (small operations - general surgery - high assistance surgery)
- ISO 5: 3500/ m^3 particles
- ISO 7: 350000/ m^3 particles

Characteristics	Operating theatre		
	Very high air quality	High air quality	Standard air quality
Temperature (C°)	Winter ≥ 20 Summer ≤ 24		
Relative Humidity (%)	Winter ≥ 40 Summer ≤ 60		
Overpressure (Pa) with respect to the outside	15		
Outside air (vol/l)	15		
Recirculation air	yes	yes	-
Cleaning classes UNI EN ISO 14644-1	ISO5	ISO7	ISO8
Final filtration level	H14		
Sound pressure level (dB)	45		

The ventilation systems in operating rooms

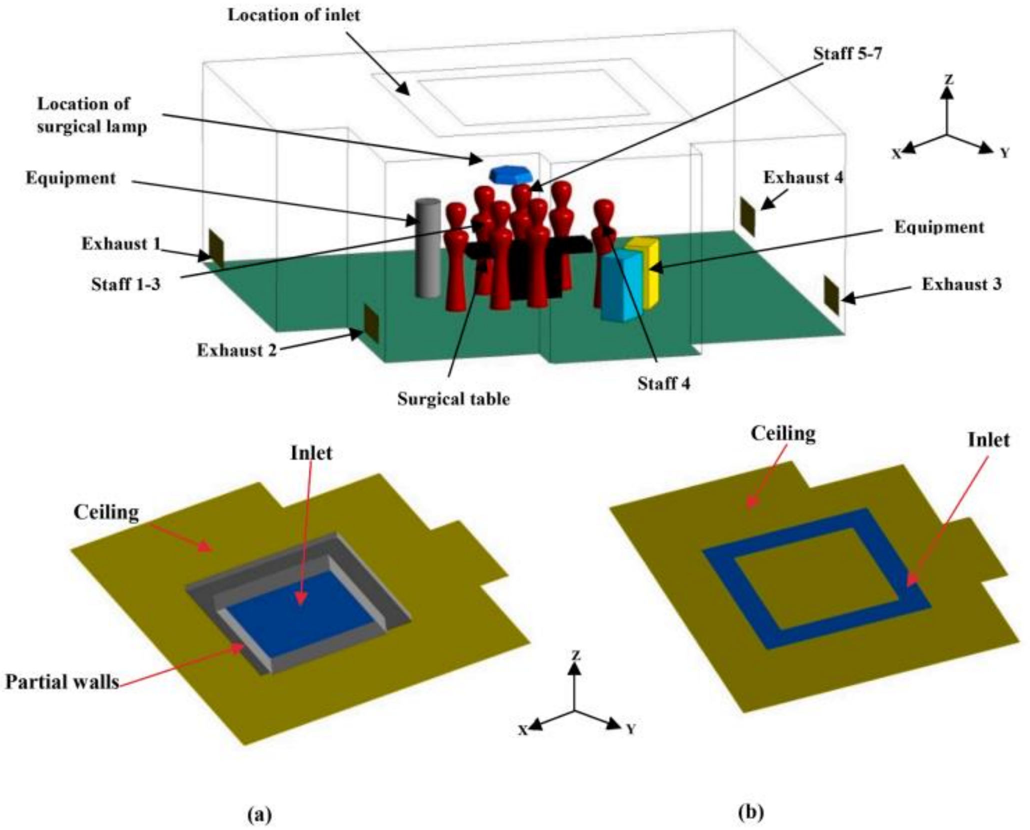

(a) UDF ventilation and (b) Mixing ventilation, Reprinted from Sadeghian [75]

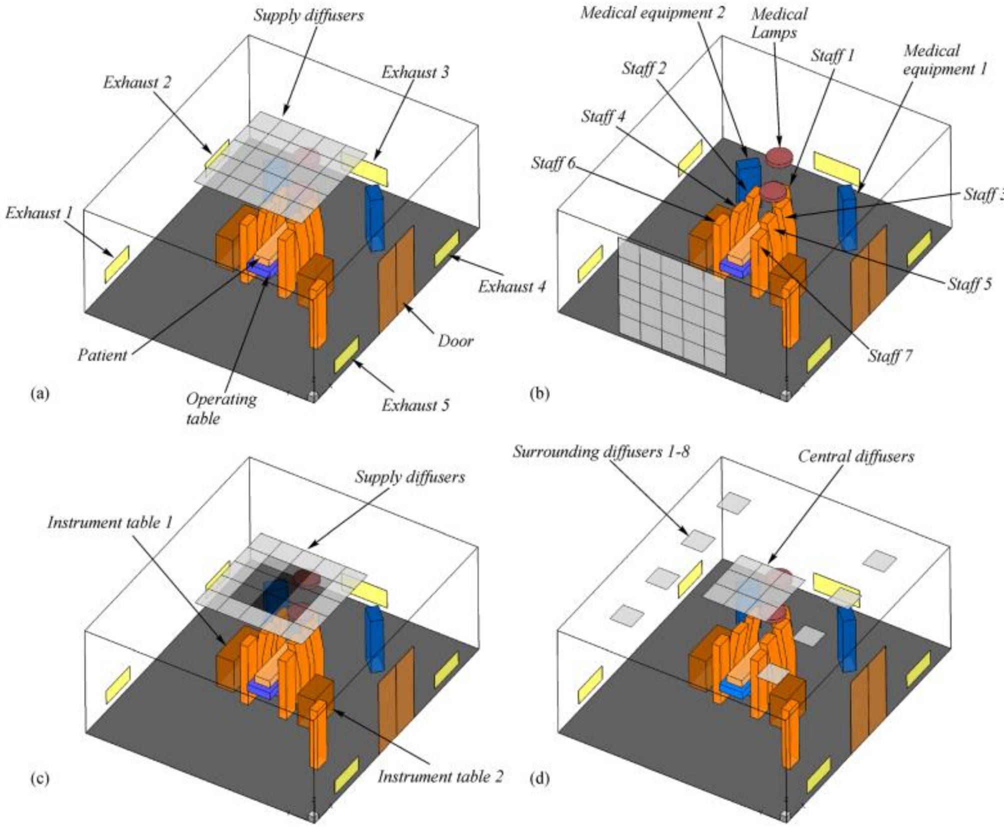

(a) VLAF, (b) HLAF, (c) DVAF, (d) TAF. Reprinted from Zhai et al. [94]

Software & tools

- Ansys Space Claim and Design Modeler to release:
  - the geometry

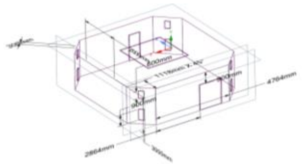

- Fluent Meshing to realized:
  - the mesh

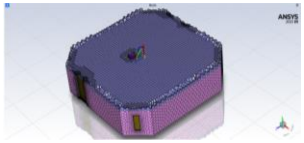

- RBF Morph to obtain:
  - the change position of cylinder/human dummy and in the next steps the change of the ventilation system kind in the operating theatre and the different angle/position of surgical lamps

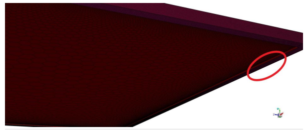

- Workbench to obtain:
  - the points of DoE (Design of Experiment)

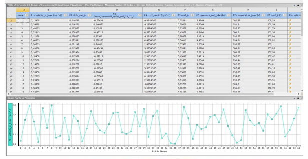

- Fluent to study:
  - the fluid dynamic field and obtain
  - the snapshots

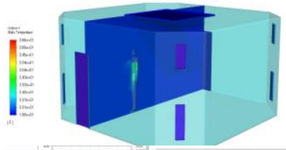

- Twin Builder to created and export:
  - the ROM (Reduced Order Model)
  - The Digital Twin

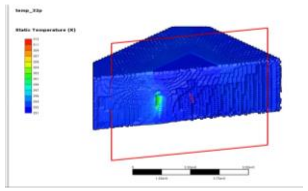

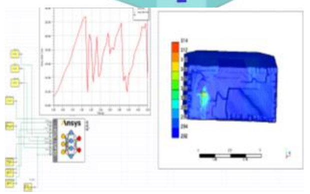

- Mathematica Wolfram to evaluate:
  - the quantities for vapor H_2O

Case study: the S. Gerardo operating theatre

The geometry is the one of the San Gerardo Hospital in Monza: geometry of a room with a central HVAC system of surface ($6.25 m^2$) and 8 discharge grilles, 4 upper 4 lower

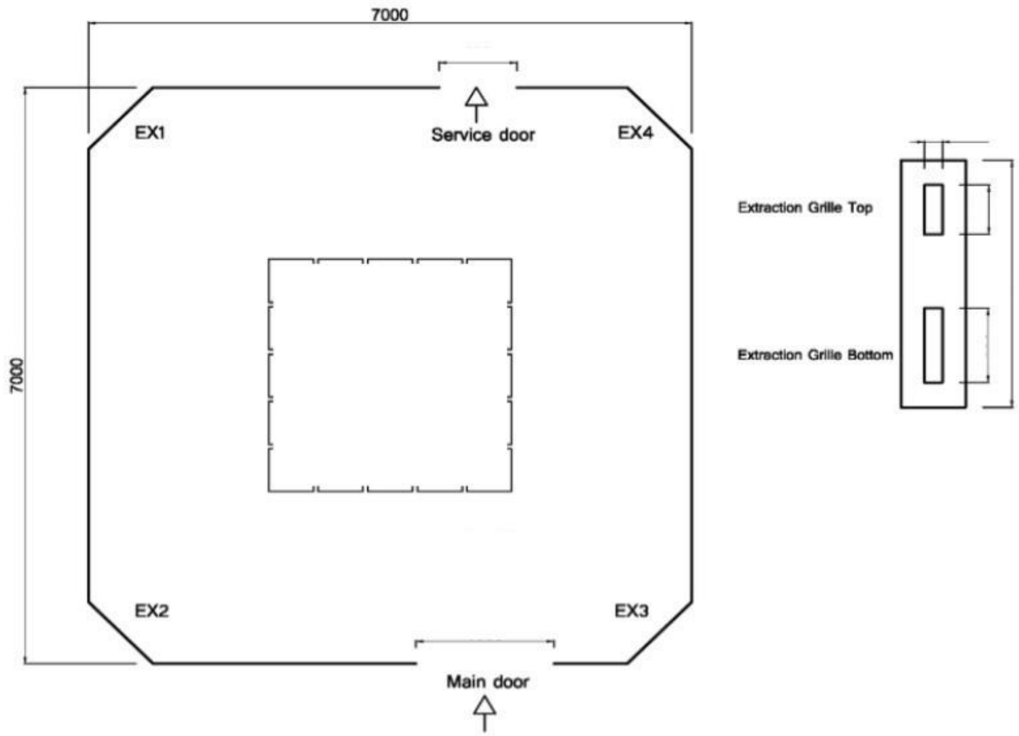

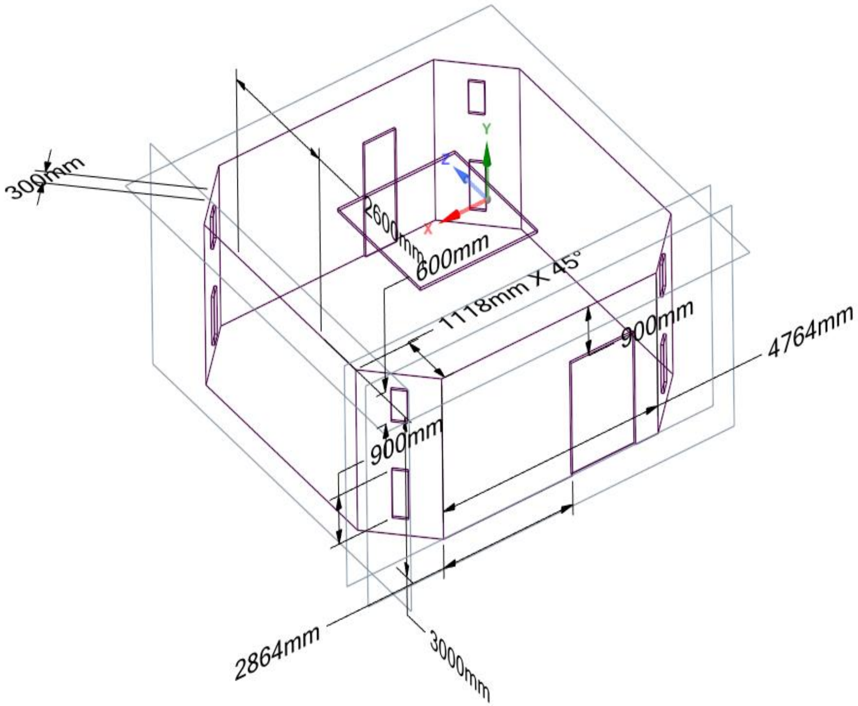

The S. Gerardo operating theatre : CFD setup

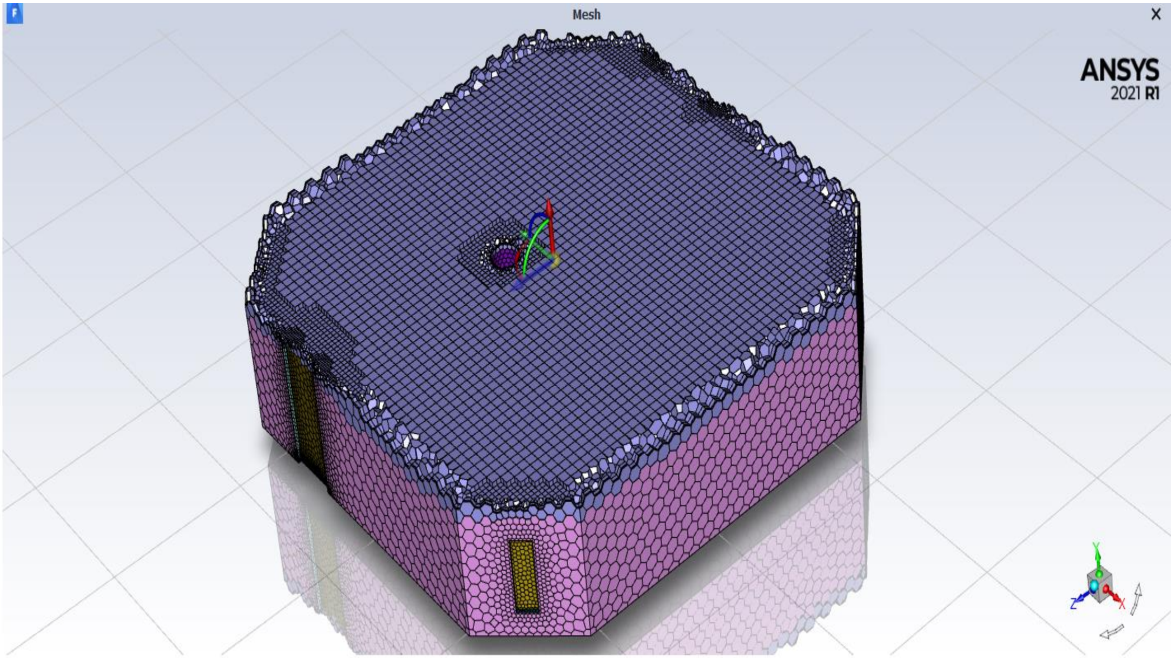

- Steady state simulations with a pseudo-time step
- Energy equation
- Turbulence term: standard k-ε with wall function
- B.C
  - Isothermal wall room
  - Human dummy wall non-adiabatic
  - Velocity inlet
  - Pressure outlet

Operating theatre model with cylindrical dummy

The geometry has been discretized with 300k poly-hexa elements

The **medical staff** is represented with a **cylindrical dummy:**

- h=1.8m and d=0.4m
- with a thermal flux equal to 45 W/ m^2

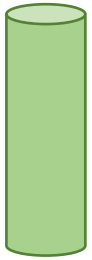

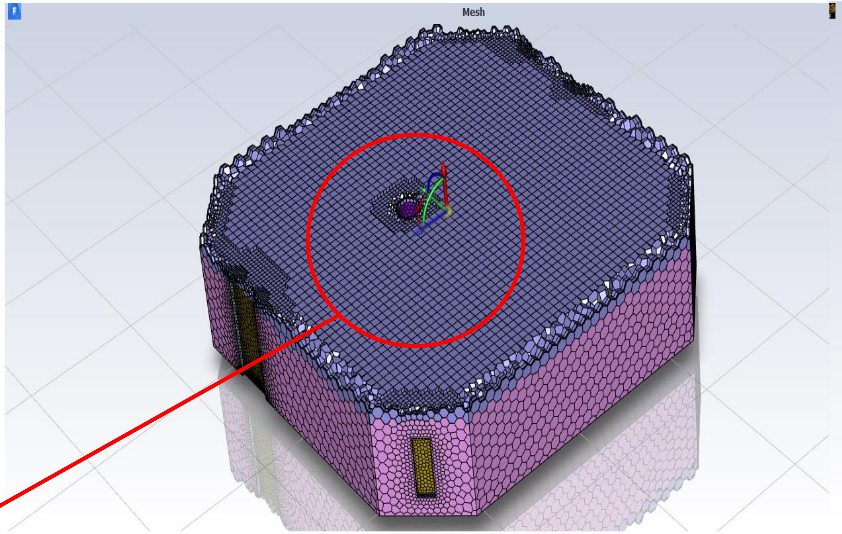

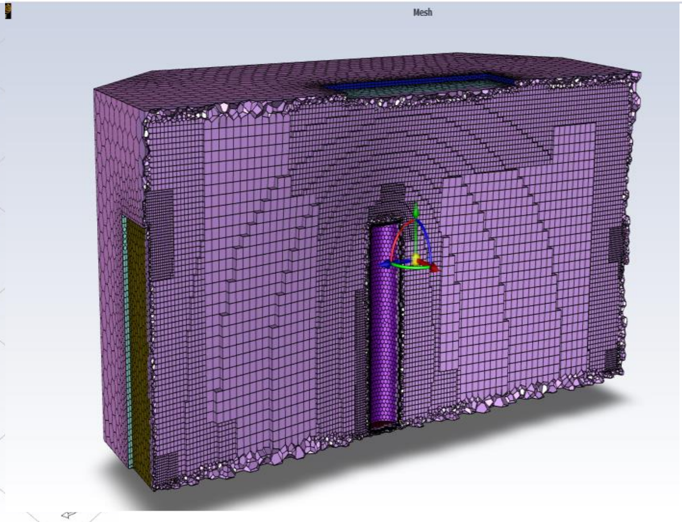

Boundary and Initial Conditions	
Temperature room	298,1K
Temperature inlet HVAC	293,1K
Pressure	1 atm
Velocity inlet HVAC	0,3 m/s

	Room size	HVAC size	Wall	Top size exhaust grilles	Bottom exhaust grilles size
	7x7x3 (m)	2,5x2,5 (m)	Steel	0,6x0,3 (m) n.ro 4	0,9x0,3 (m) n.r 4

The S. Gerardo with cylindrical dummy: results (1/2)

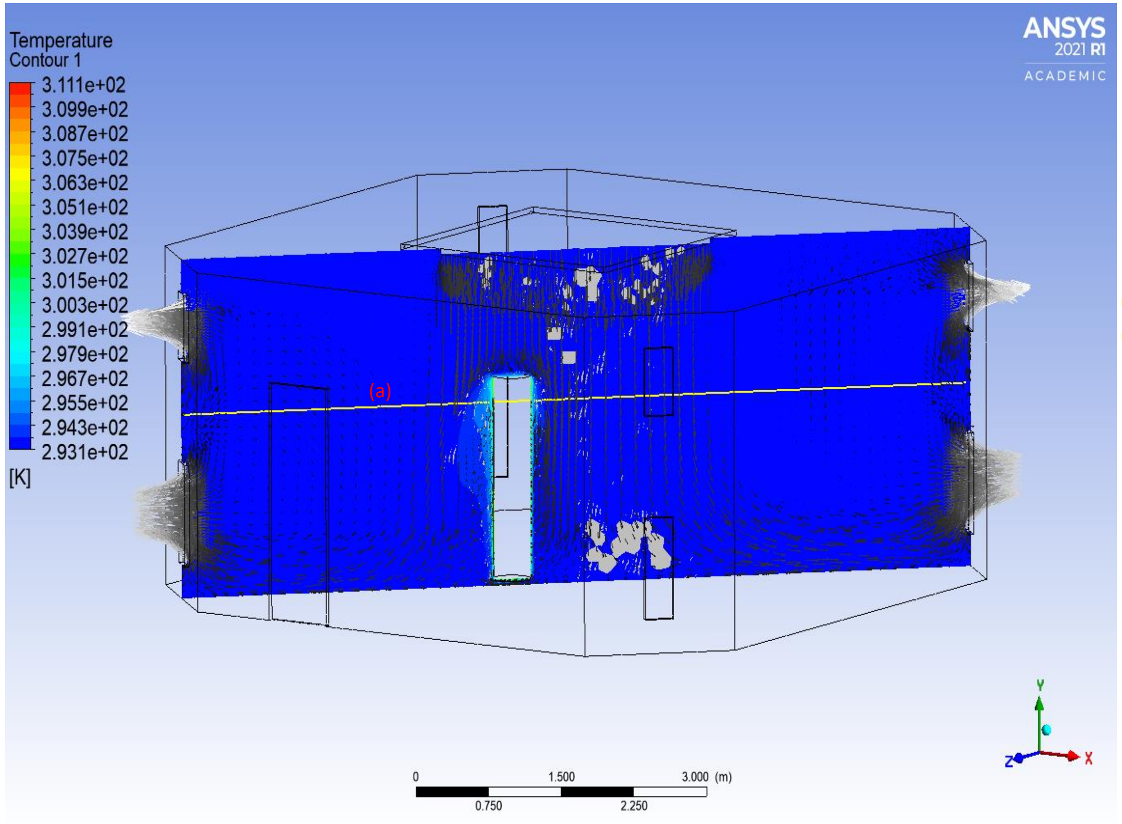

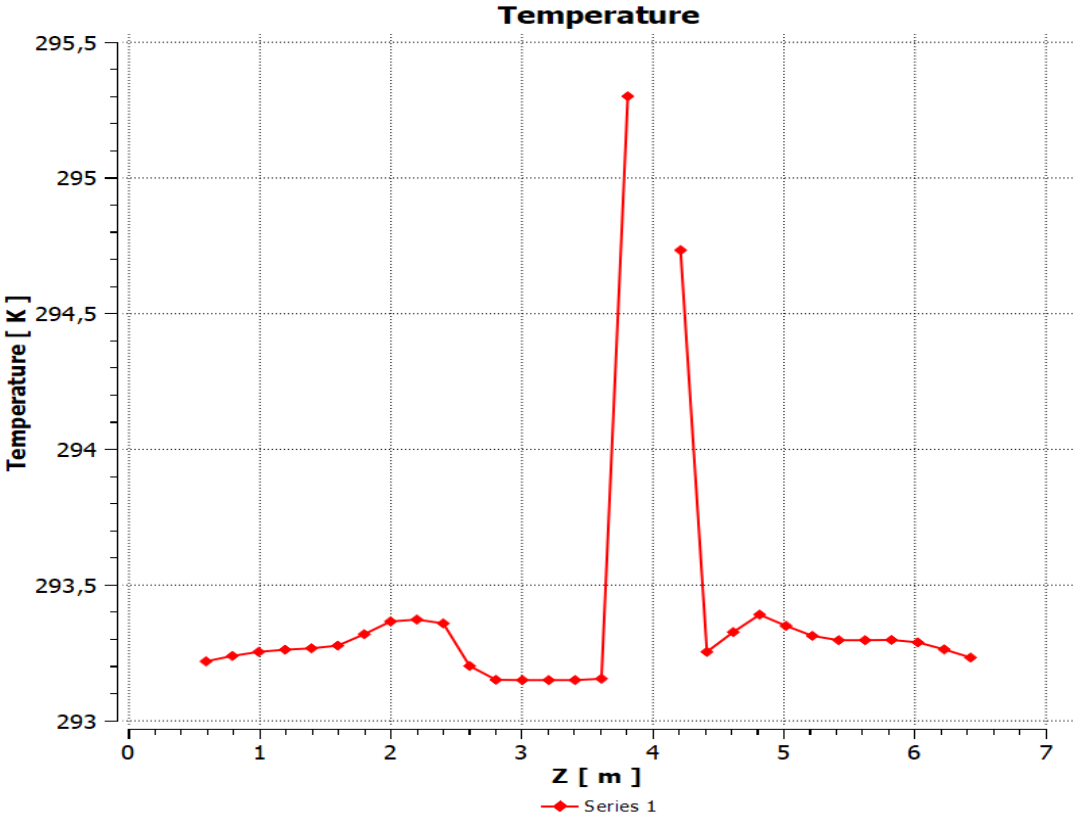

- On the left, the temperature field with superimposed velocity vector field
- On the right, temperature trend in 30 points extracted along the line on the diagonal section of the chamber

The S. Gerardo with cylindrical dummy: results (2/2)

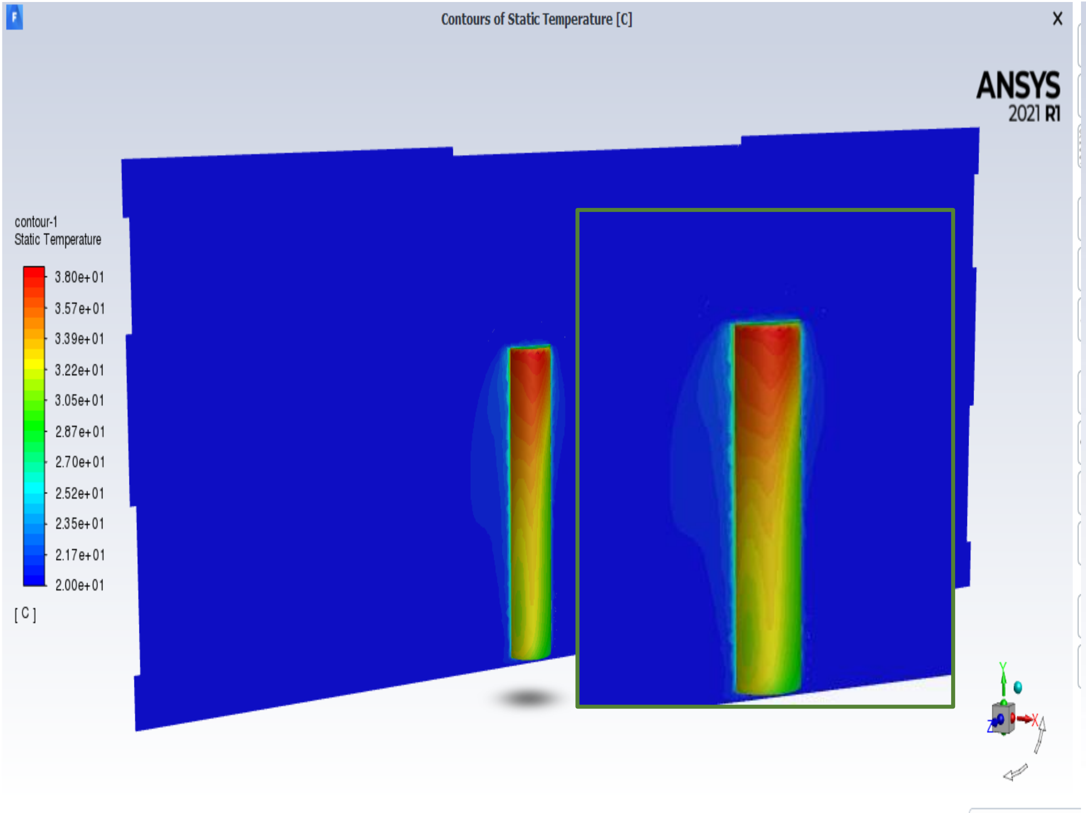

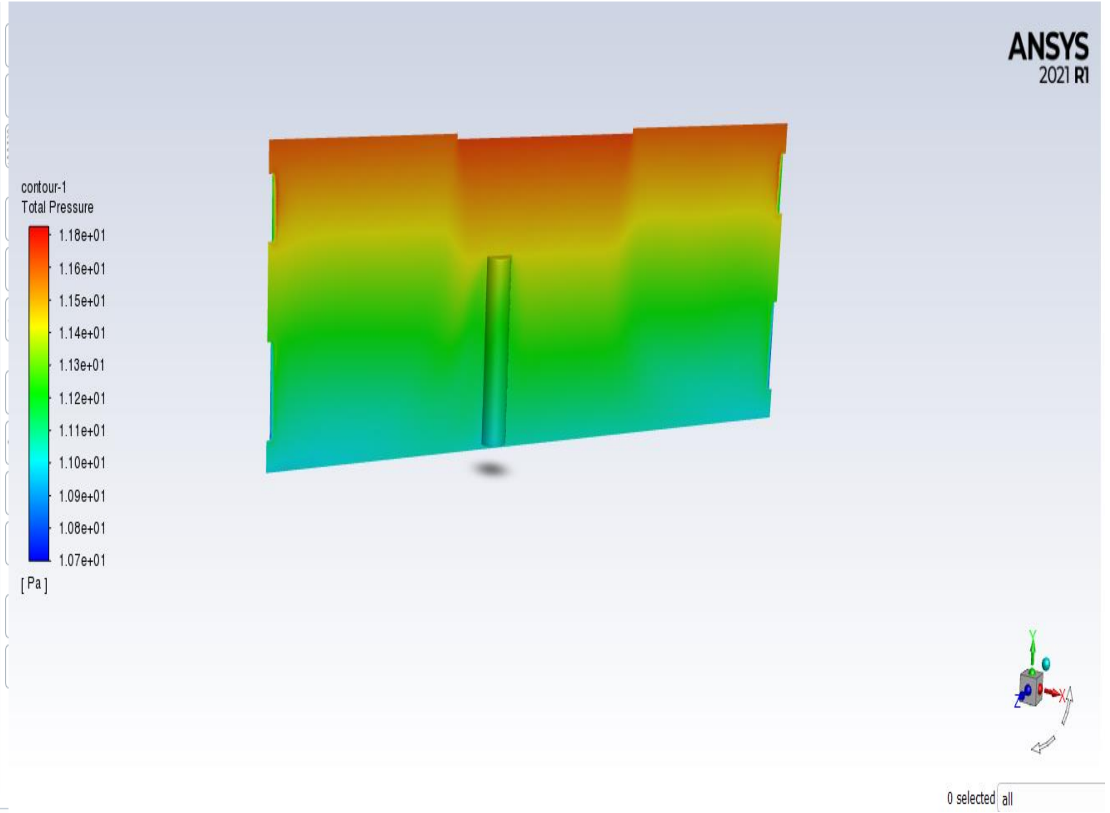

- Temperature field and details according to the diagonal plane and according to an yz plane
- Evolution of the pressure field on the diagonal section of the operating theatre: the field appears stratified showing an overpressure near the ceiling. This trend is in agreement with that indicated in Sanchez [79]

Operating theatre model with human dummy

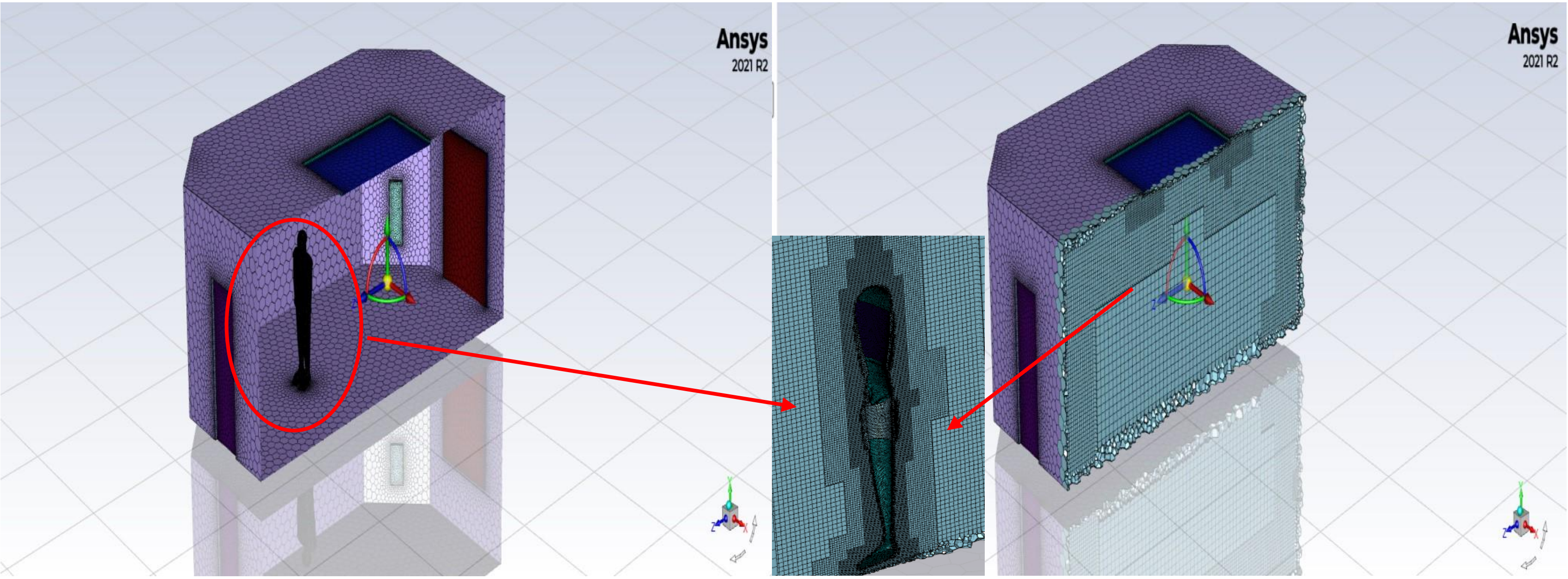

Initial Conditions	
Temperature room	298,15
Pressure [Pa]	101325

Variation range of parameters		
Parameters	Min values	Max value
Velocity [m/s]	0,1	0,5
Temperature [K]	291,15	310,15
Δ Pressure [Pa]	2,0	8
Molar fraction H2O	0,010	0,031
Position human dummy [m]	-1,0	1,0

The geometry was discretized with 3.3 mil poly-hexa elements, 5.7 mil nodes.

	Operating theatre size	HVAC size	Wall	Top size exhaust grilles	Bottom size exhaust grilles
Case study with human dummy	7x7x3 (m)	2,5x2,5 (m)	Still	0,6x0,3 (m) n.ro 4	0,9x0,3 (m) n.ro 4

Operating theatre model with human dummy & CO_2

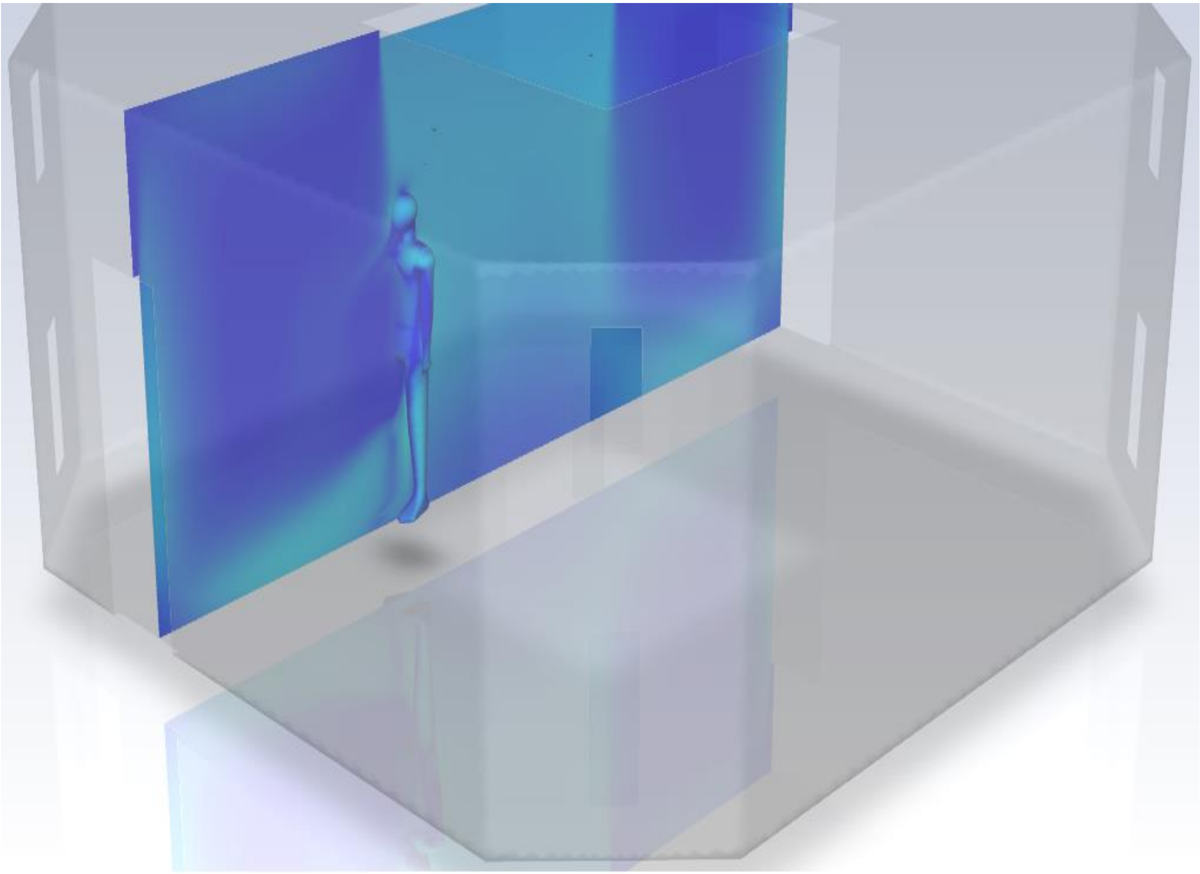

The new model includes:

- the **new parameters** are the **mole fraction** of H_2O vapor to evaluate the **relative humidity,** and **mass fraction** of CO_2 which considers the exhalation phase during respiration

- the CO_2 is inserted as a boundary condition (a front the mouth) in terms of the volumetric flow rate of the emission and mass fraction.

- the amount of CO_2 inserted in exhalation is about 80l/h Balocco et al. and [15] Cheng et al. [28].

- the **mole fraction** of H_2O vapor

- the power given on the human dummy is **117.0 W** and the heat flux **is 52.9 W/** m^2

ROM setup

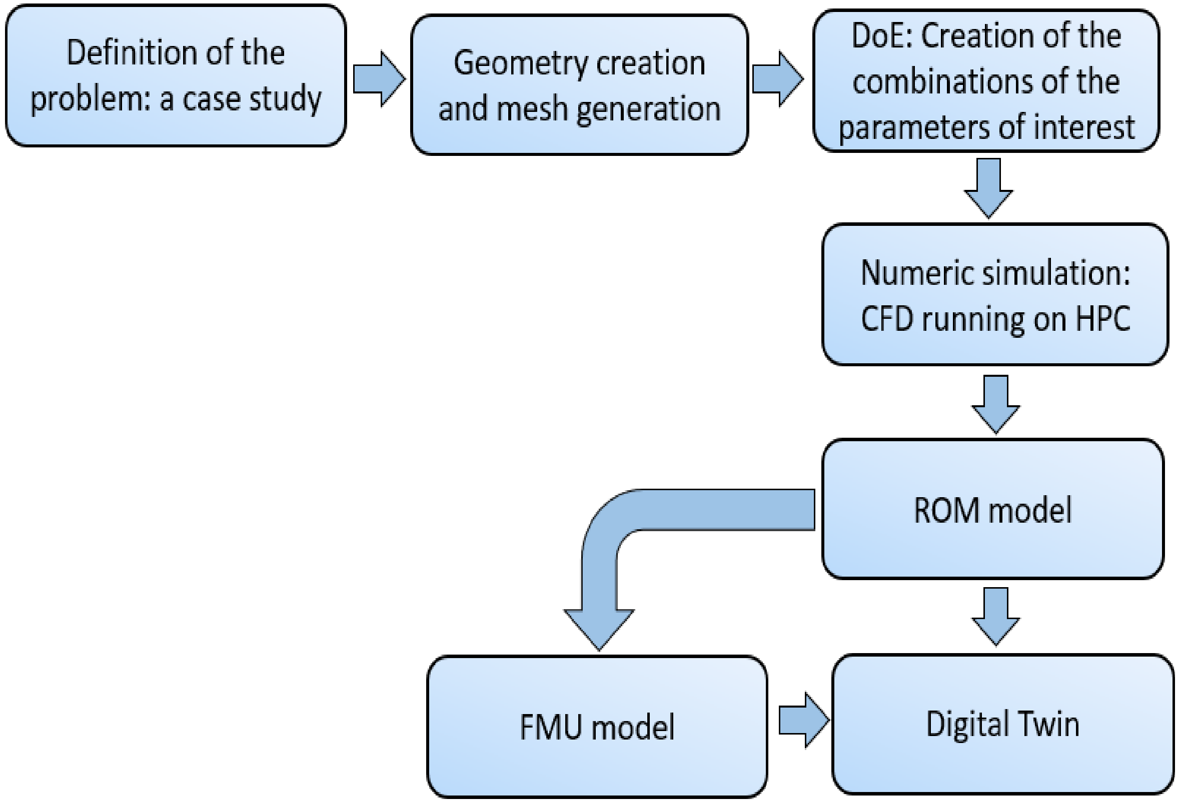

- ➢Steady ROM
- ➢Split set snapshots in learning and validation sets
- ➢SVD algorithm
- ➢GARS (Genetic Aggregation Response Surface) algorithm
- ➢Evaluation of ROM relative errors and reduction errors
- ➢Validation
- ➢Integration between parameter and shape variations
- ➢Export ROM to build the digital twin

Design of Experiment (DoE) and ROM (1/2)

Rows 1 samples: all values of parameters in the defined range of samples
Columns 1 parameters: parameters used to build the ROM

Rows and Columns 2: trend between the **minimum** and **maximum** of the **different input parameters** for **all** samples and for **all** parameters

Columns: Parameters (8)

Rows: Samples (64)

Table of Schematic B2: Design of Experiments (Optimal Space-Filling Design : Max-Min Distance : Maximum Number Of Cycles = 10 : User-Defined Samples : Random Generator Seed = 0 : Number of Samples = 64)

	A	B	C	D	E	F	G	H	I	
1	Name	P1 - velocity_in_hvac (m s^-1)	P2 - h2o_vap_in	P3 - Geom_humanoid3_outlet_co2_23_07_d...	P4 - co2_mouth (kg s^-1)	P5 - co2_in	P6 - pressure_out_grille (Pa)	P7 - temperature_hvac (K)	P8 - co2_t (K)	P9 - velocity
2	1	0,13438	0,014298	-0,73438	4,9719E-05	0,75391	5,9844	302,88	309,29	
3	2	0,34688	0,016256	0,046875	4,2856E-05	0,79609	6,7344	291,6	300,54	
4	3	0,49063	0,027022	0,10938	3,5994E-05	0,23359	6,3594	297,53	301,79	
5	4	0,32813	0,030937	-0,45313	6,5731E-05	0,45859	6,6406	300,2	302,26	
6	5	0,12188	0,020823	0,26563	4,3619E-05	0,90859	3,1719	293,38	302,88	
7	6	0,46563	0,025391	0,078125	6,4206E-05	0,36016	4,9531	299,61	309,92	
8	7	0,26563	0,021149	0,54688	2,4556E-05	0,37422	2,6094	293,67	302,1	
9	8	0,49688	0,013972	-0,48438	3,3706E-05	0,52891	5,8906	308,81	305,85	
10	9	0,16563	0,022454	0,73438	3,8281E-05	0,61328	7,6719	308,22	307,26	
11	10	0,18438	0,015929	-0,57813	2,9131E-05	0,43047	2,4219	307,03	307,42	
12	11	0,37188	0,030284	-0,26563	2,2269E-05	0,89453	5,2344	296,94	303,82	
13	12	0,14688	0,010709	0,57813	2,5319E-05	0,72578	4,3906	302,28	304,6	
14	13	0,39063	0,023759	-0,51563	5,3531E-05	0,14922	2,7969	307,92	304,13	
15	14	0,33438	0,013319	0,29688	6,3444E-05	0,83828	3,4531	293,08	306,63	
16	15	0,12813	0,019844	-0,76563	6,1919E-05	0,68359	6,4531	294,86	303,35	
17	16	0,25938	0,012341	-0,95313	2,9894E-05	0,81016	4,2969	295,75	303,51	
18	17	0,43438	0,028001	0,32813	4,8956E-05	0,69766	5,4219	309,7	301,63	
19	18	0,30938	0,028979	0,98438	5,5819E-05	0,78203	6,1719	296,64	302,73	
20	19	0,24063	0,024738	-0,85938	3,0656E-05	0,26172	5,3281	292,19	303,2	

1

Samples vs Parameters

Parameters Parallel Chart

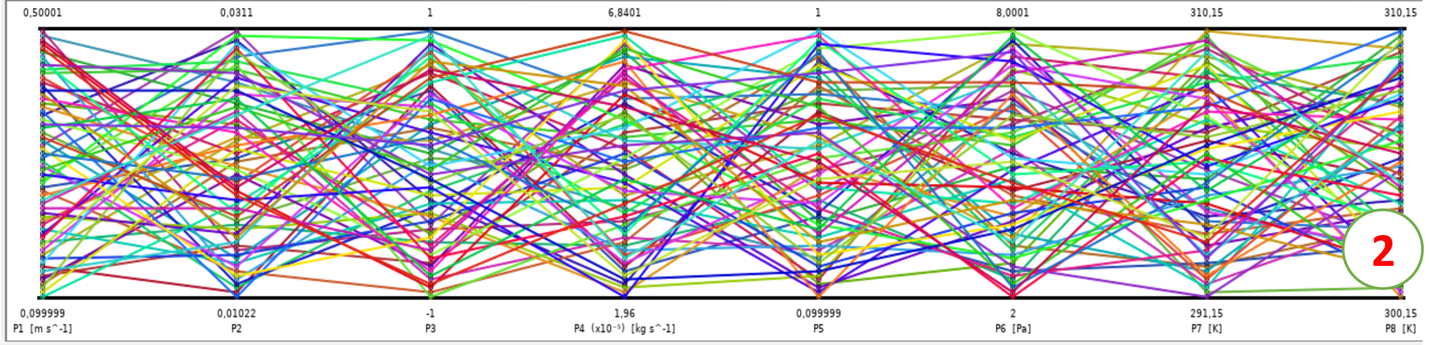

Design of Experiment (DoE) and ROM (2/2)

Columns: Parameters (8)

Rows 1 samples: all values of parameters in the defined range of samples
Columns 1 parameters: parameters used to build the ROM

Rows and Columns 2: trend between the **minimum** and **maximum** of **one between the input parameters** with respect to the **number of samples**

Rows: Samples (64)

1 Parameter vs samples

Table of Schematic B2: Design of Experiments (Optimal Space-Filling Design : Max-Min Distance : Maximum Number Of Cycles = 10 : User-Defined Samples : Random Generator Seed = 0 : Number of Samples = 64)

	A	B	C	D	E	F	G	H	I	
1	Name	P1 - velocity_in_hvac (m s^-1)	P2 - h2o_vap_in	P3 - Geom_humanoid3_outlet_co2_23_07_d...	P4 - co2_mouth (kg s^-1)	P5 - co2_in	P6 - pressure_out_grille (Pa)	P7 - temperature_hvac (K)	P8 - co2_t (K)	P9 - velocit
2	1	0,13438	0,014298	-0,73438	4,9719E-05	0,75391	5,9844	302,88	309,29	
3	2	0,34688	0,016256	0,046875	4,2856E-05	0,79609	6,7344	291,6	300,54	
4	3	0,49063	0,027022	0,10938	3,5994E-05	0,23359	6,3594	297,53	301,79	
5	4	0,32813	0,030937	-0,45313	6,5731E-05	0,45859	6,6406	300,2	302,26	
6	5	0,12188	0,020823	0,26563	4,3619E-05	0,90859	3,1719	293,38	302,88	
7	6	0,46563	0,025391	0,078125	6,4206E-05	0,36016	4,9531	299,61	309,92	
8	7	0,26563	0,021149	0,54688	2,4556E-05	0,37422	2,6094	293,67	302,1	
9	8	0,49688	0,013972	-0,48438	3,3706E-05	0,52891	5,8906	308,81	305,85	
10	9	0,16563	0,022454	0,73438	3,8281E-05	0,61328	7,6719	308,22	307,26	
11	10	0,18438	0,015929	-0,57813	2,9131E-05	0,43047	2,4219	307,03	307,42	
12	11	0,37188	0,030284	-0,26563	2,2269E-05	0,89453	5,2344	296,94	303,82	
13	12	0,14688	0,010709	0,57813	2,5319E-05	0,72578	4,3906	302,28	304,6	
14	13	0,39063	0,023759	-0,51563	5,3531E-05	0,14922	2,7969	307,92	304,13	
15	14	0,33438	0,013319	0,29688	6,3444E-05	0,83828	3,4531	293,08	306,63	
16	15	0,12813	0,019844	-0,76563	6,1919E-05	0,68359	6,4531	294,86	303,35	
17	16	0,25938	0,012341	-0,95313	2,9894E-05	0,81016	4,2969	295,75	303,51	
18	17	0,43438	0,028001	0,32813	4,8956E-05	0,69766	5,4219	309,7	301,63	
19	18	0,30938	0,028979	0,98438	5,5819E-05	0,78203	6,1719	296,64	302,73	
20	19	0,24063	0,024738	-0,85938	3,0656E-05	0,26172	5,3281	292,19	303,2	

1

Design Points vs Parameter

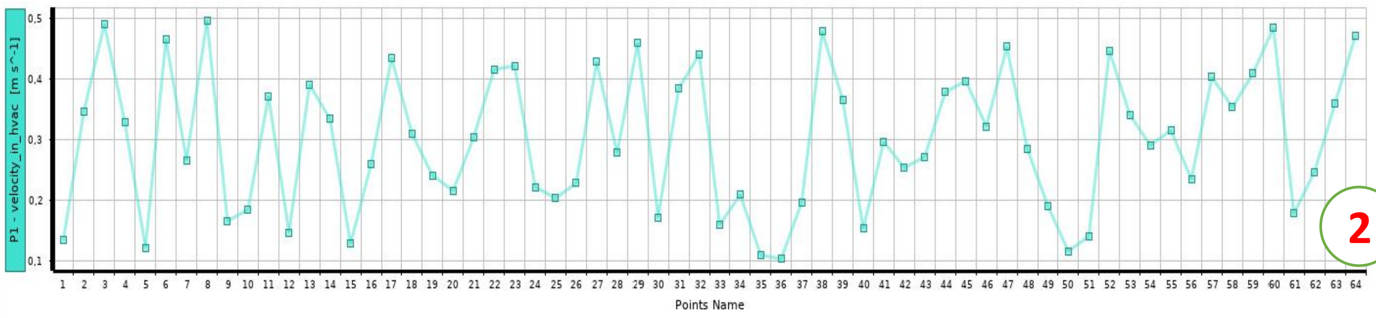

2

ROM vs ROM

In the **construction** of the **ROM**, they are considered **relevant**:

- **Relative Reduction Error:** the ratio between the difference of the reference solution of each field snapshot and the projection with respect to the reference solution. The error varies according to the number of modes chosen.

$$RRE = \frac{\|X_{ref} - X_{proj}\|}{\|X_{ref}\|}$$

- **ROM Relative Error**: includes both reduction and interpolation errors.

$$ROMRE = \frac{\|X_{ref} - X_{ROM}\|}{\|X_{ref}\|}$$

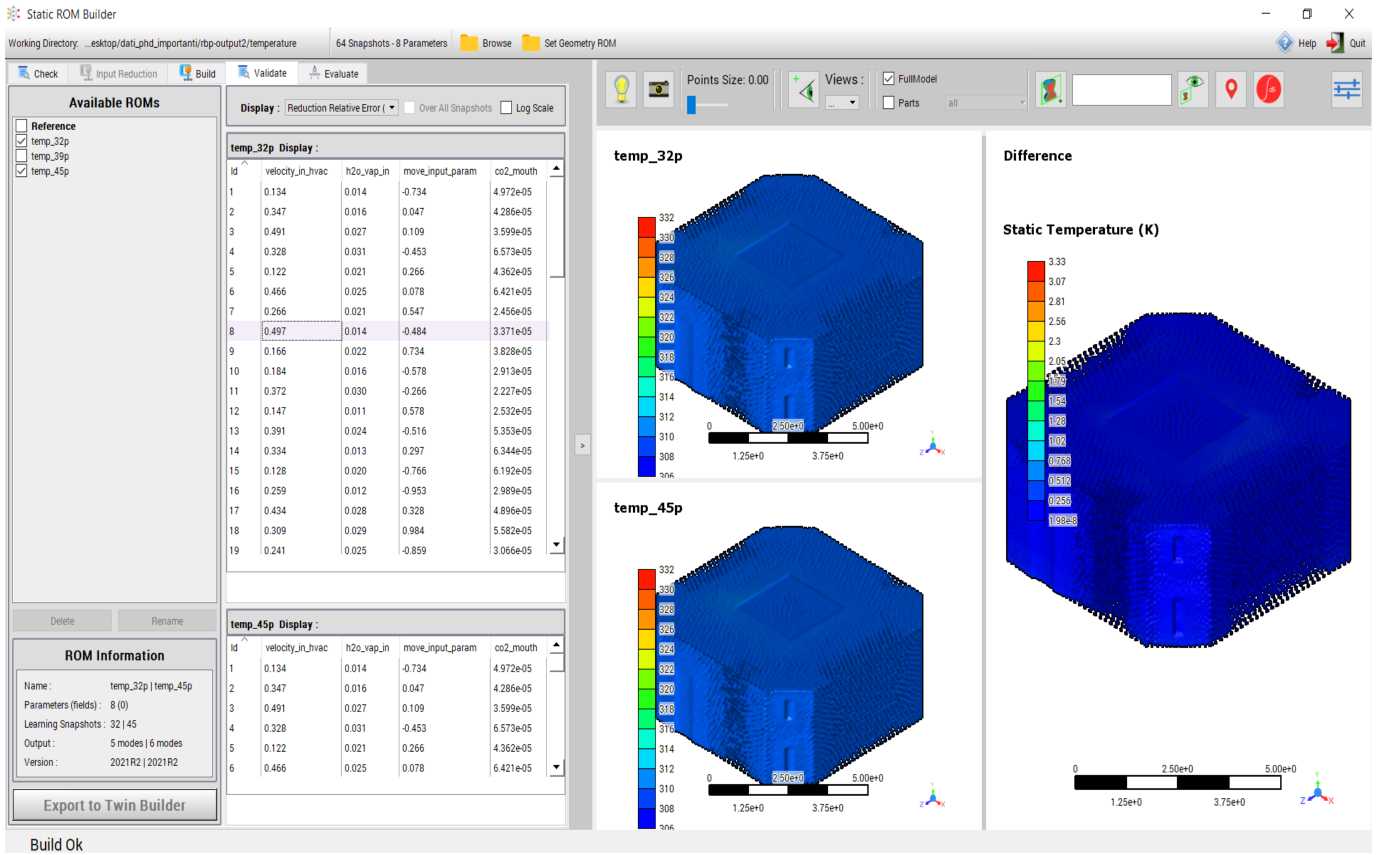

Temperature field: the difference between ROMs built by the same set of snapshots but with a different number of snapshots (32 and 45) to obtain it.

CFD vs ROM: Temperature comparison (1/2)

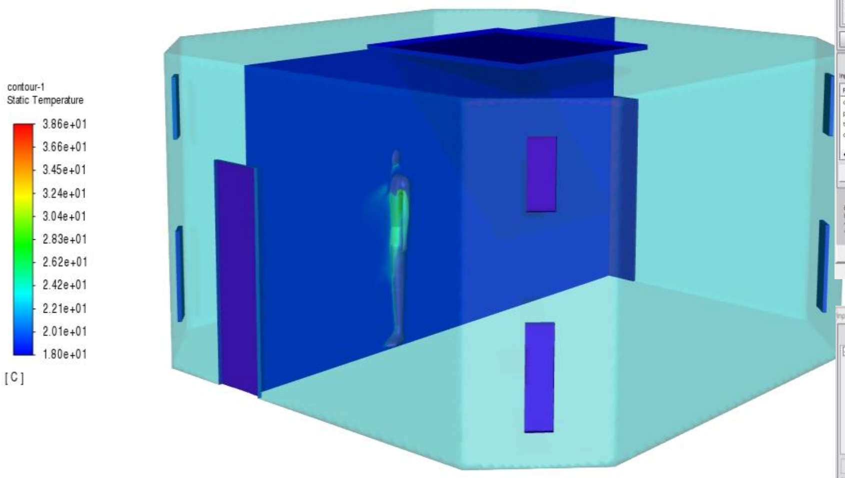

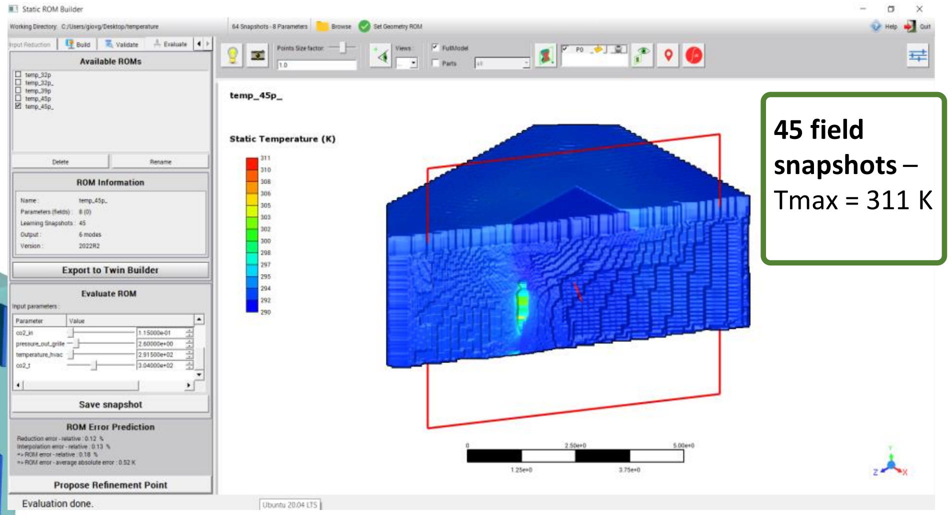

45 field snapshots – Tmax = 311 K

Comparison of **CFD** (left) and **ROM** (right) results constructed with 70% of the different set of snapshots (64 snapshots). The temperature range is underestimated by about 1,9%

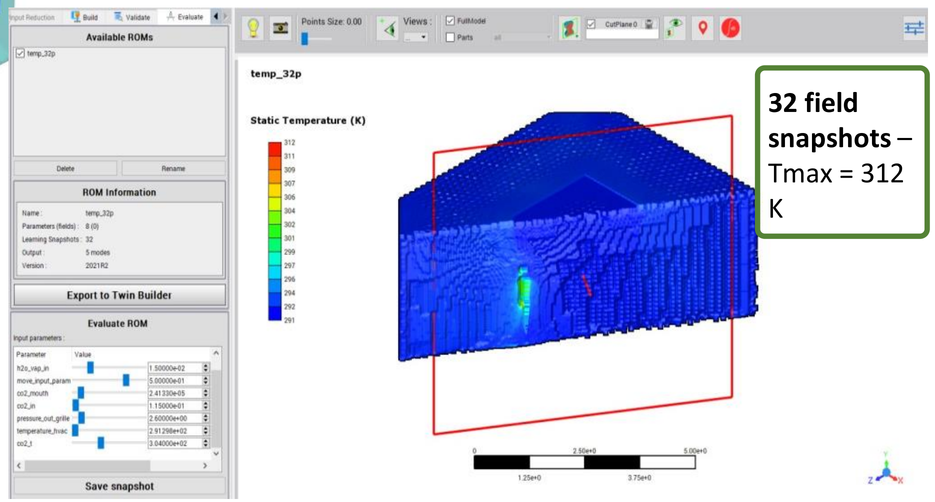

32 field snapshots – Tmax = 312 K

Comparison of **CFD** (left) and **ROM** (right) results constructed with 50% of the different set of snapshots (64 snapshots). The variation of the temperature field between CFD and ROM is underestimated by about 0.64%.

CFD vs ROM: Temperature comparison (2/2)

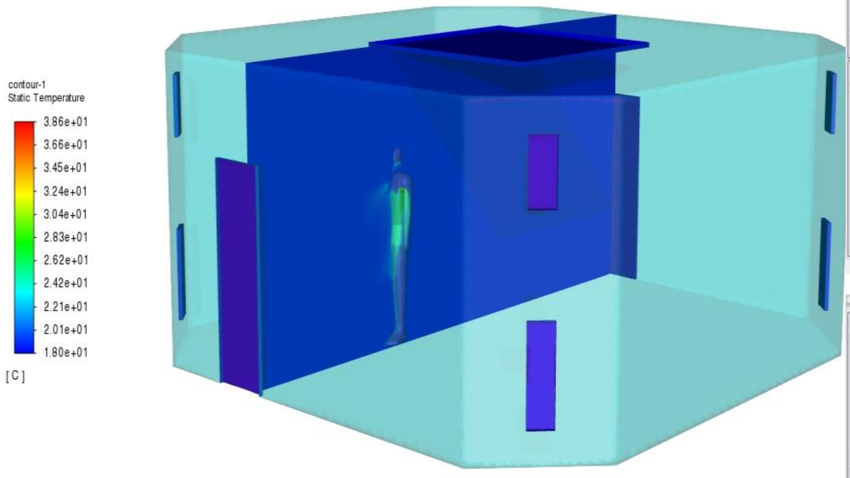

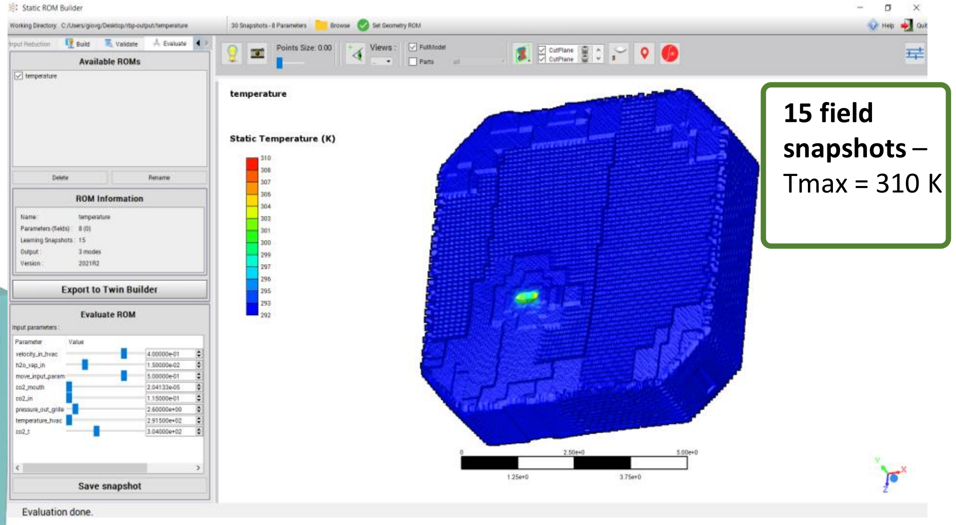

15 field snapshots – Tmax = 310 K

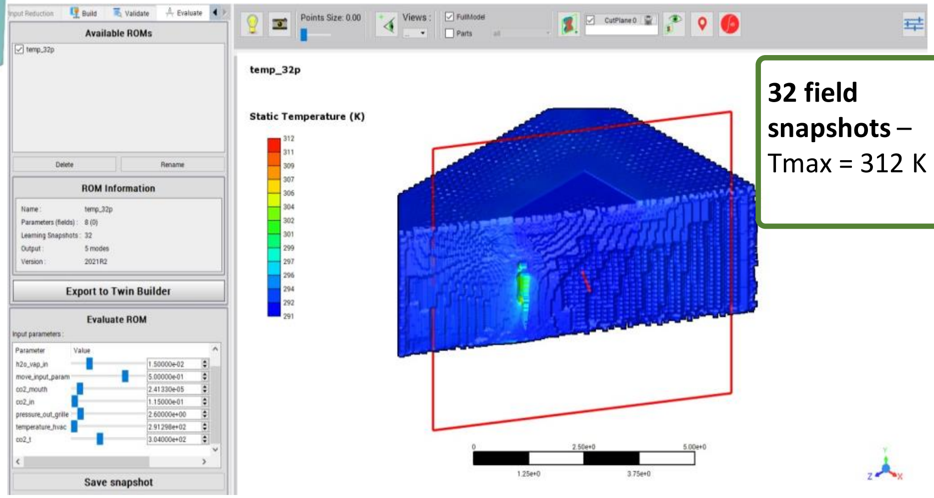

32 field snapshots – Tmax = 312 K

Comparison of **CFD** (left) and **ROM** (right) results constructed with 50% of the different set of snapshots (**30 snapshots**). The temperature range is underestimated by about 5%

Comparison of **CFD** (left) and **ROM** (right) results constructed with 50% of the different set of snapshots (**64 snapshots**). The variation of the temperature field between CFD and ROM is underestimated by about 0.64%.

CFD vs ROM Relative Humidity: comparison

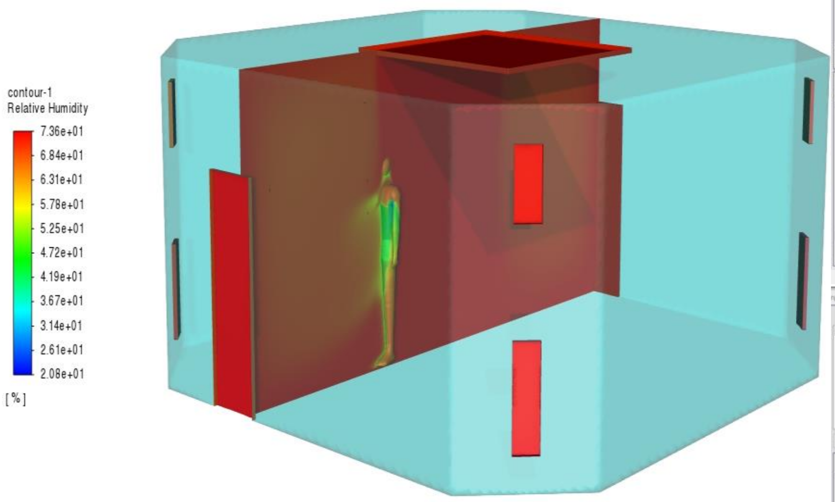

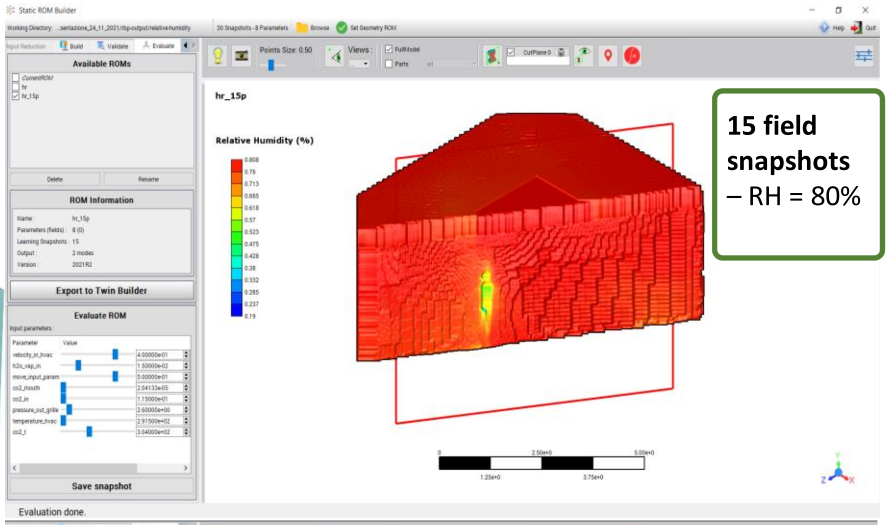

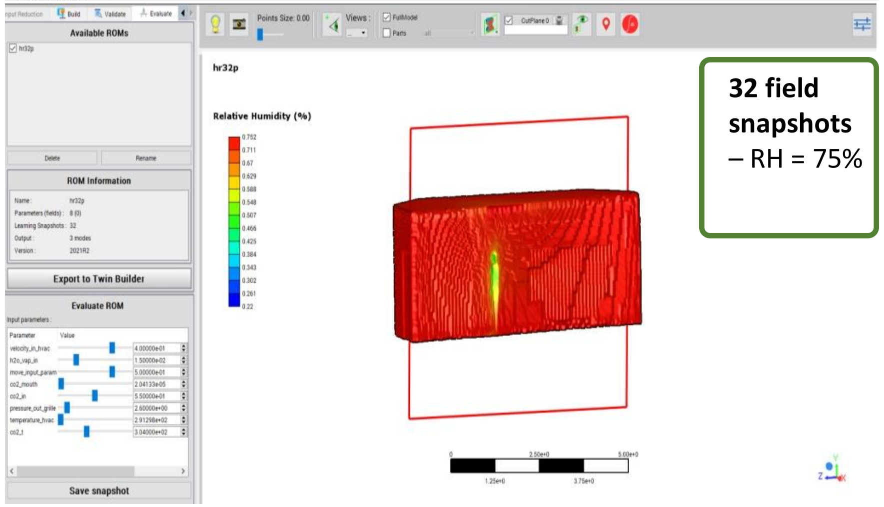

The optimal amount of relative humidity is 50% and 60%.
Comparison of **CFD** (left) and **ROM** (right) results made with 50% field snapshots. The relative humidity range is overestimated by less than 9%

Comparison of **CFD** (left) and **ROM** (right) results constructed with 50% of the different field snapshots. The variation of the temperature field between CFD and ROM is overestimated by about 2%

ROM with physical parameters change

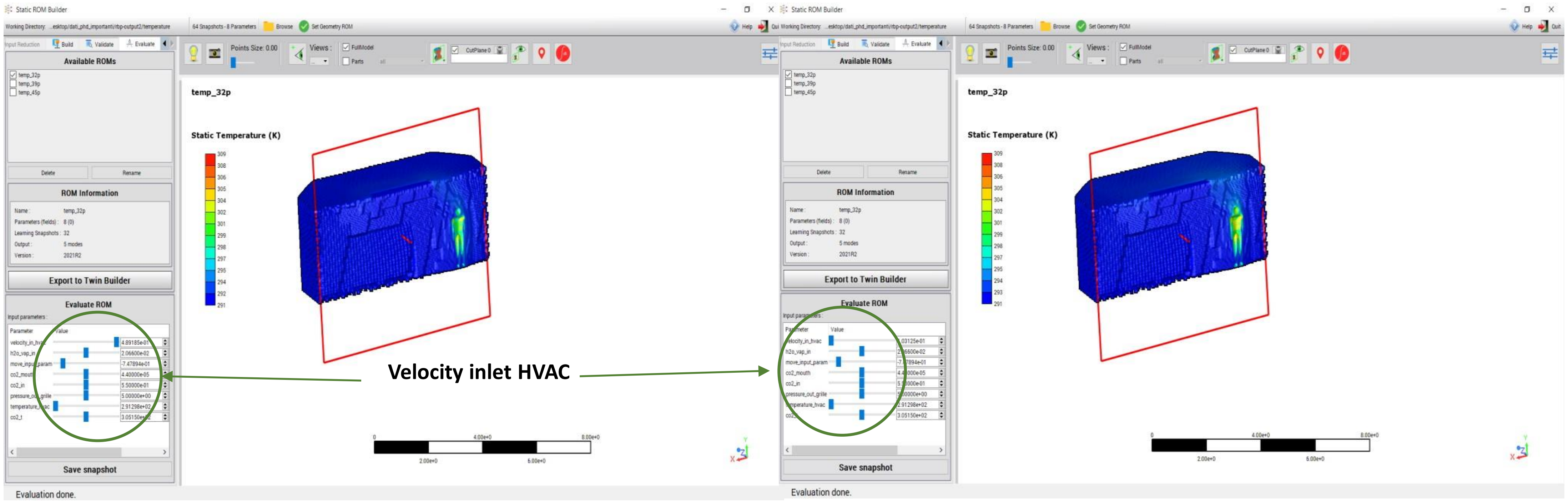

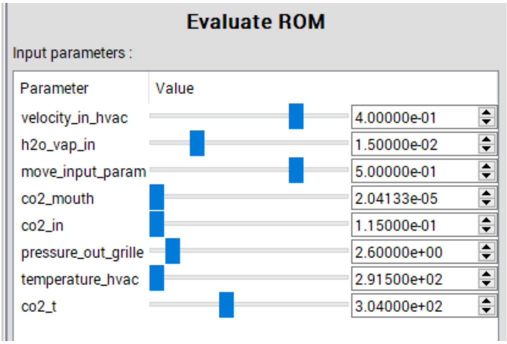

Variation of the temperature field upon changing the flow input speed only

ROM with geometrical parameters change

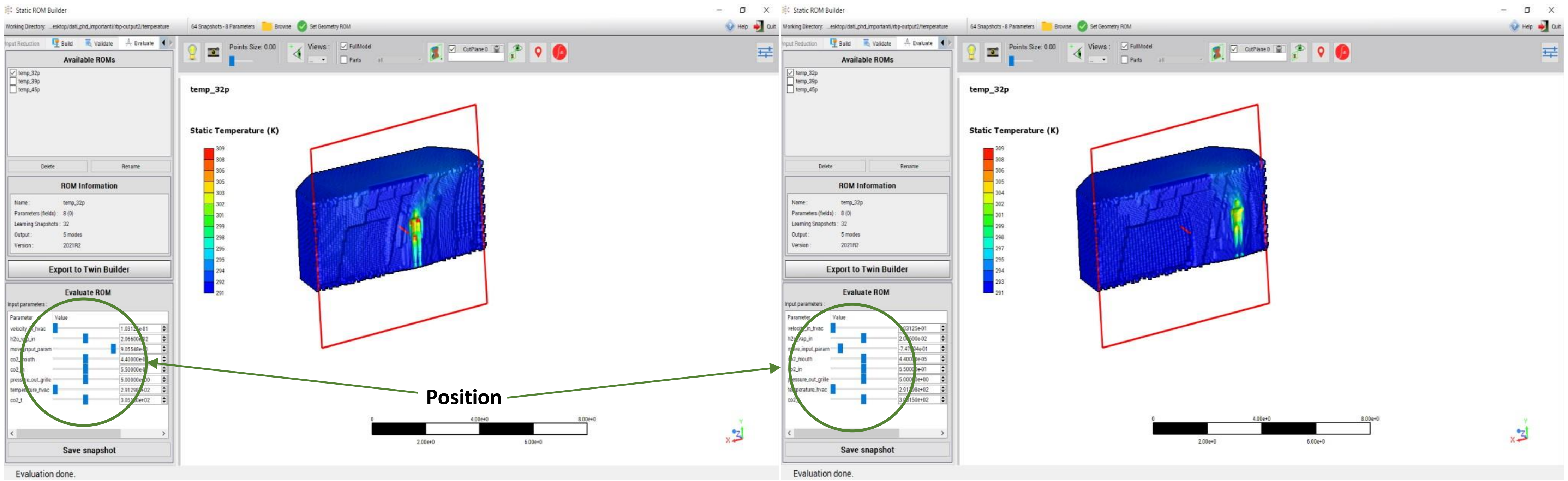

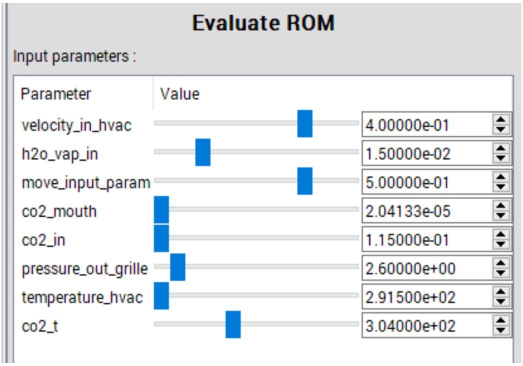

Evaluate ROM

Input parameters :

Parameter	Value
velocity_in_hvac	4.00000e-01
h2o_vap_in	1.50000e-02
move_input_param	5.00000e-01
co2_mouth	2.04133e-05
co2_in	1.15000e-01
pressure_out_grille	2.60000e+00
temperature_hvac	2.91500e+02
co2_t	3.04000e+02

Variation of the temperature field upon changing the dummy's positions only.

Digital Twin

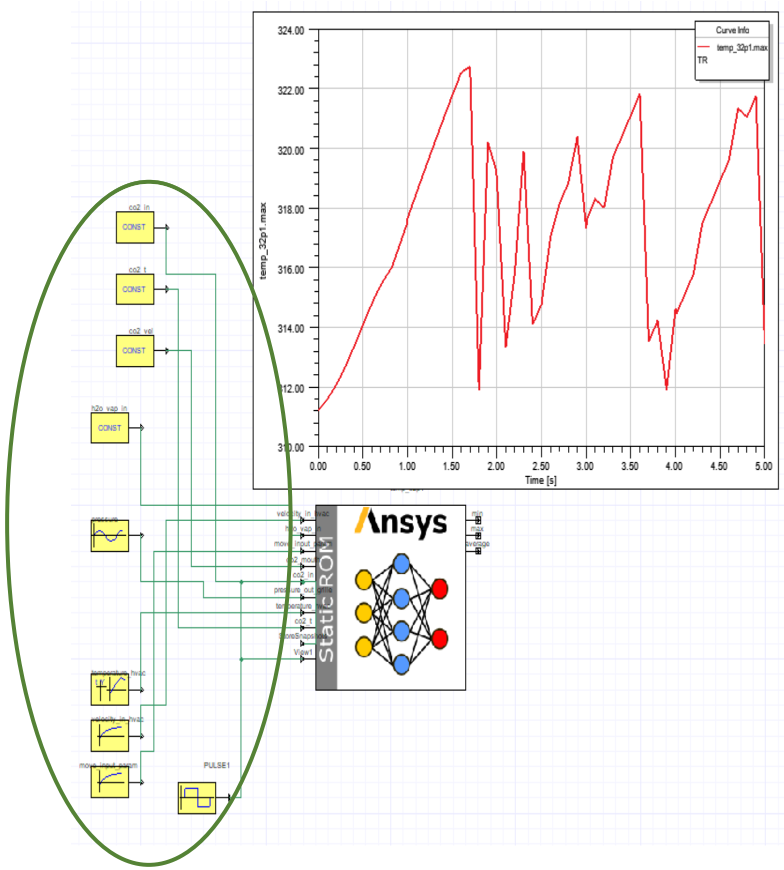

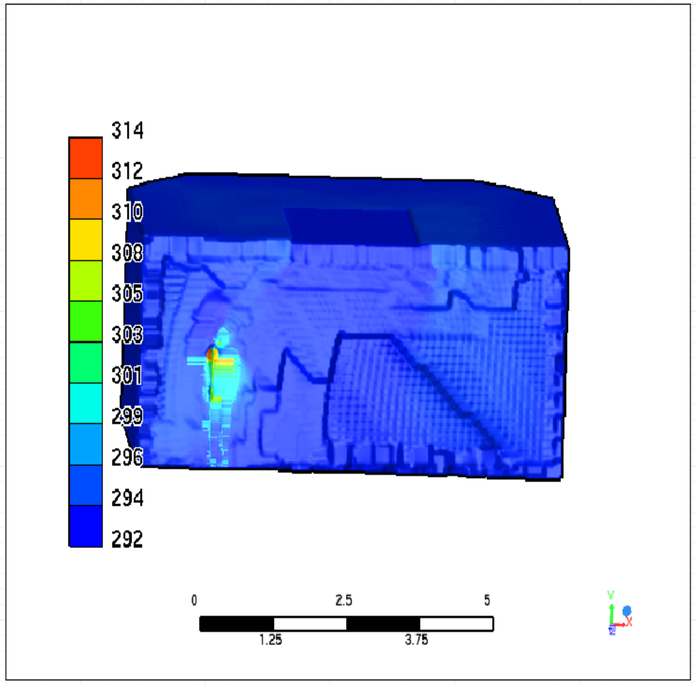

- The **ROM result** was **exported** in **TB**.
- Trend (**left**) of the **temperature** in the operating room when the input parameters change.
- **Images** (**right**) of the temperature field, in some instants in time.

S. Gerardo sub-scale model: preliminary study

Feasibility study:

- Processing feasibility:
  - Choice of scale factor

- Choice of fluid to use:
  - Possible particle tracking
    - Material to be used to simulate particles
  - Possibility of the laboratory to be able to supply the correct volumetric flow rate

- Choice of constraint:
  - Number of air changes (Air Changes Hour - ACH) to ensure air quality standards in the operating theatre
  - Analysis of the complete fluid dynamic field present in the operating theatre

S. Gerardo sub-scale model: mock-up (1/2)

1:10 scale model

Material: 10 mm thick plexiglass

- Operating Theatre
- Containment box
- Weir/bulkhead
- Box designed to have ACH≈15 and volumetric flow 18l/min
- Input of alumina particles: good buoyancy up to 10µm diameter at expected speeds
- Particle density of the order of that of the fluid (≈1 g/cm^3)

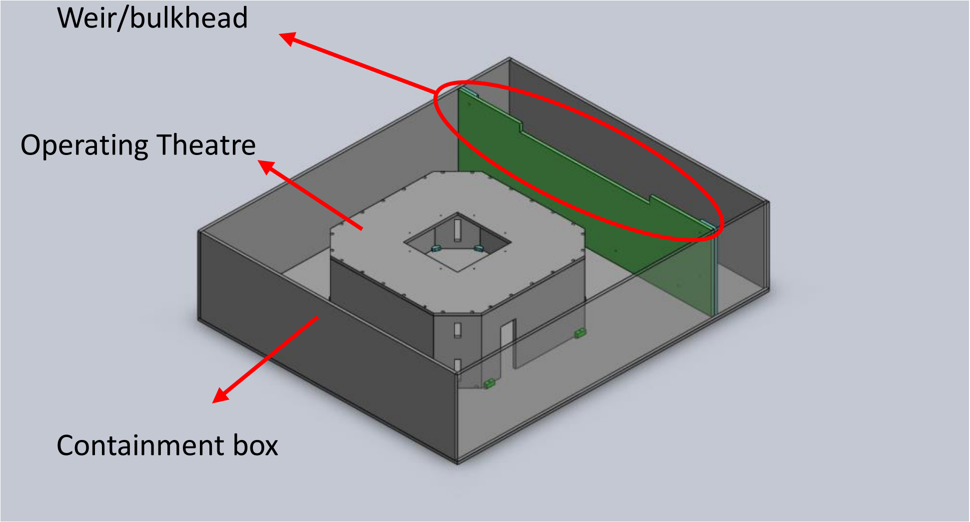

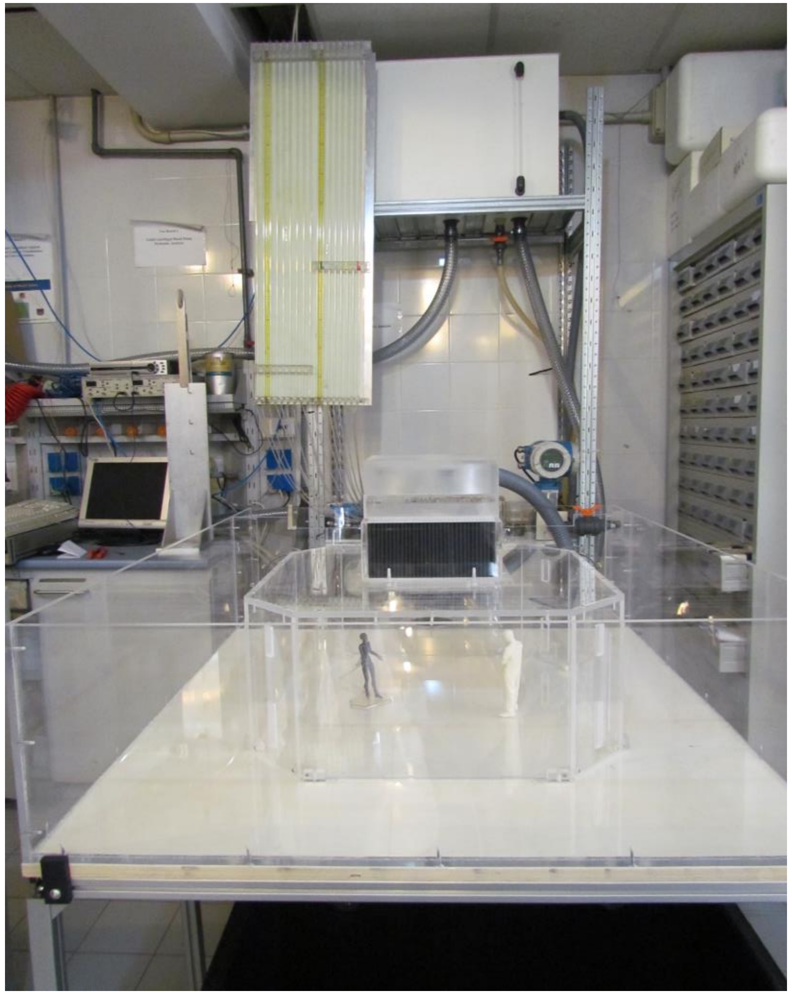

S. Gerardo sub-scale model: mock-up (2/2)

1 The scale model and three basil used to fill up the tank or to empty it

2 The tank where is highlighted the maximum level of water call as "overfull"

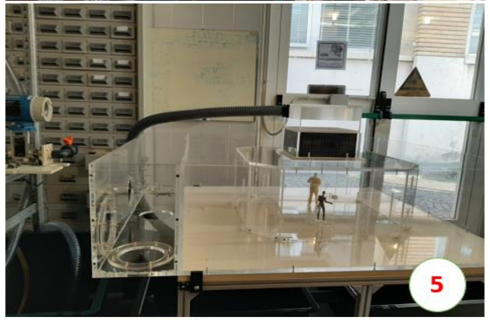

3 The pressure gauge

4 The electromagnetic flowmeter

5 The flowmeter that will be linked to the scale model

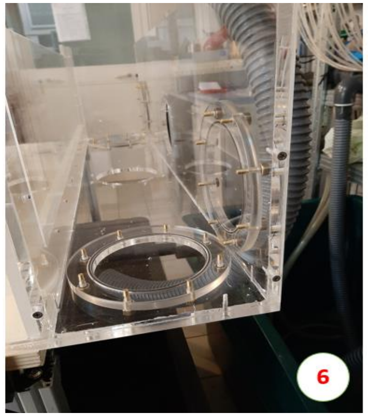

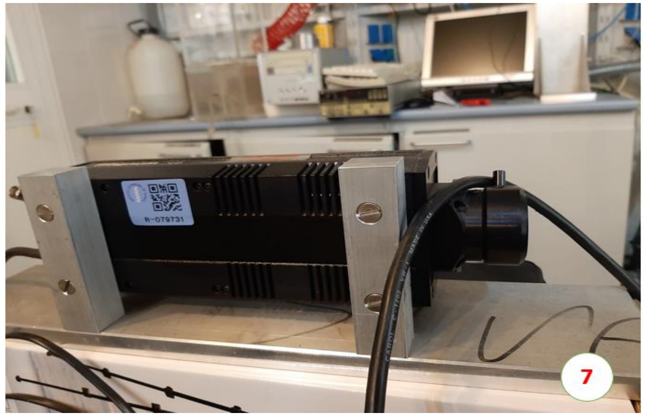

6 The holes to empty the model

7 The laser to evaluate the velocity of particles

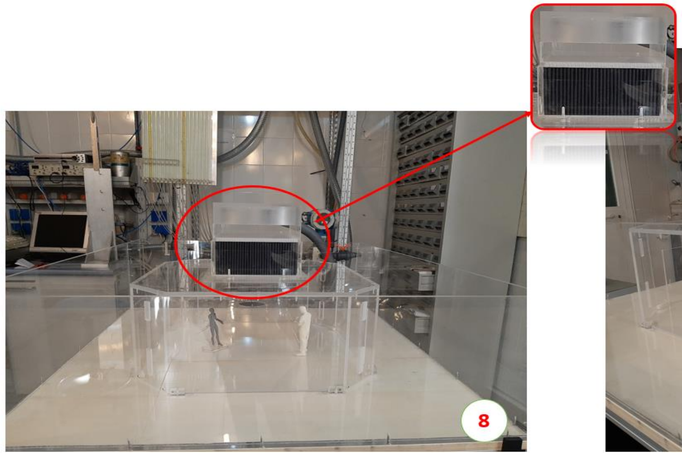

8 Mock-up made of the plexiglass material of the operating theatre

9 Zoom on the calming baffle

Beyond S. Gerardo: lamps position and size effects

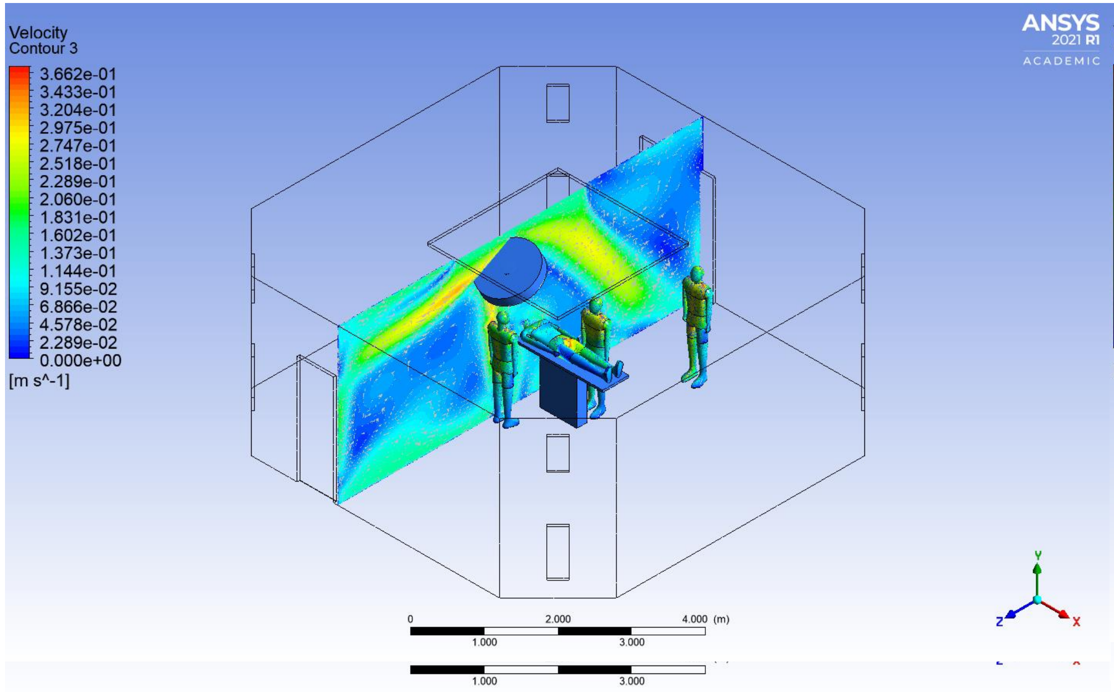

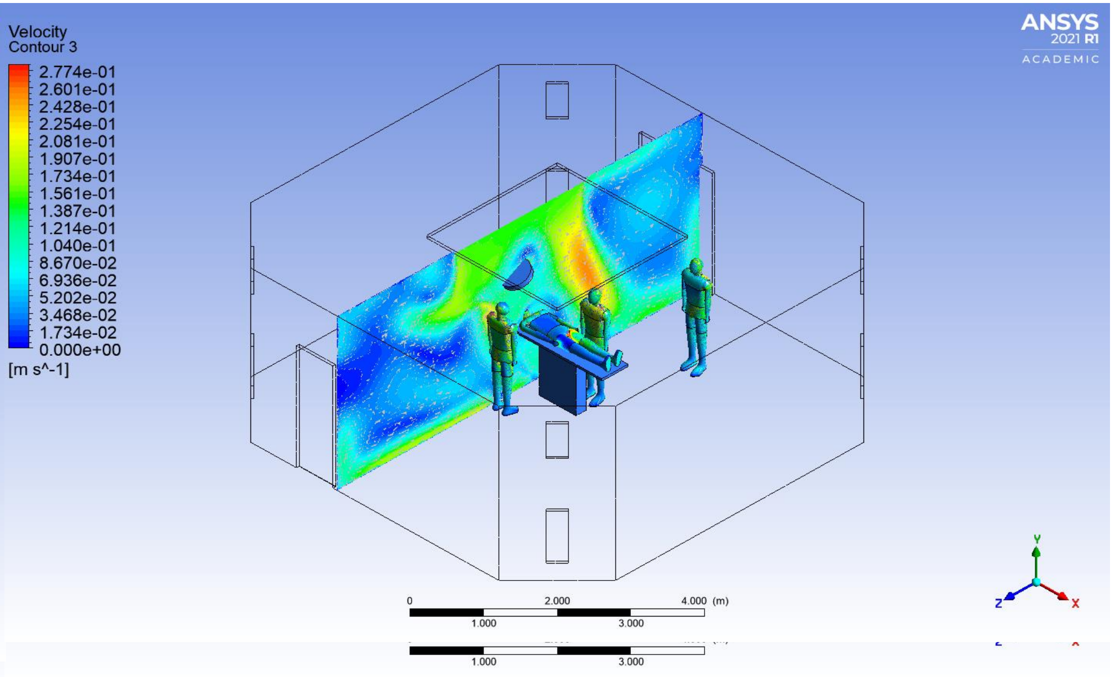

- **Complete model**: operating room with medical staff, patient, operating table, operating light, and different thermal loads for the patient and medical staff
- **Velocity field** on the YZ plane and **temperature field** on the individual dummies
- **Different sizes** of the surgical lamp, their position, and their inclination **determine** recirculation in different areas of the operating room
- In the **left** room a bigger lamp than **right** room

Complete model: lamps position and size effects (1/2)

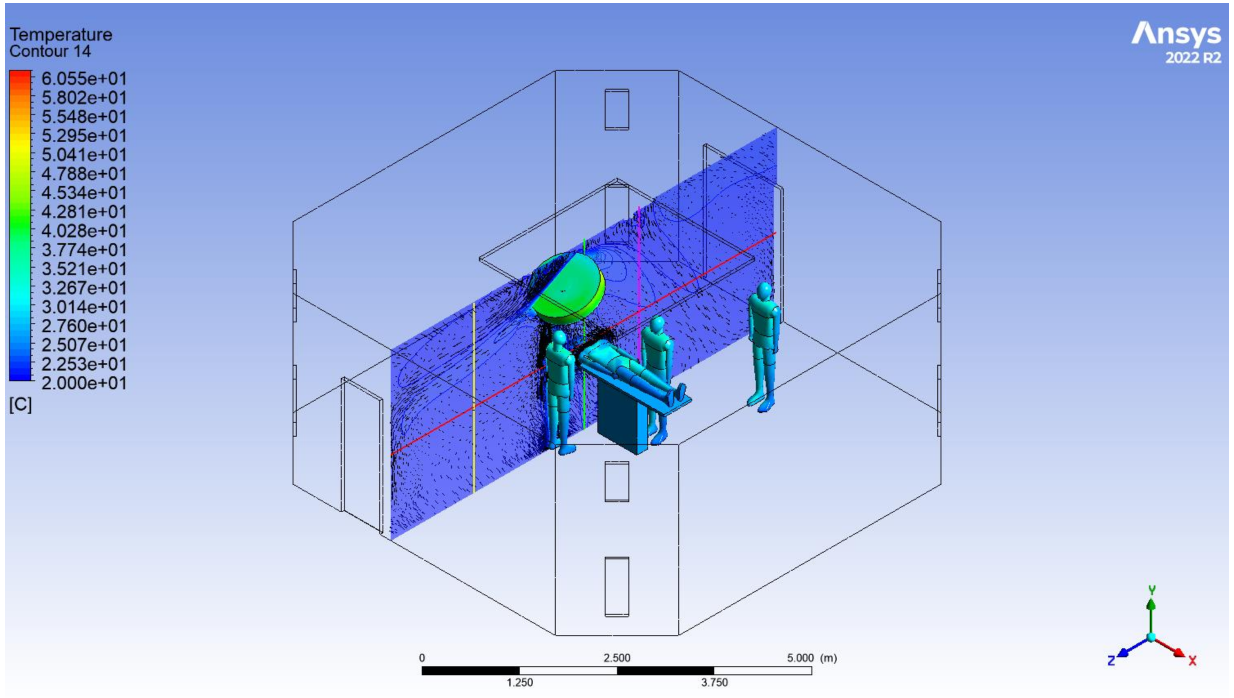

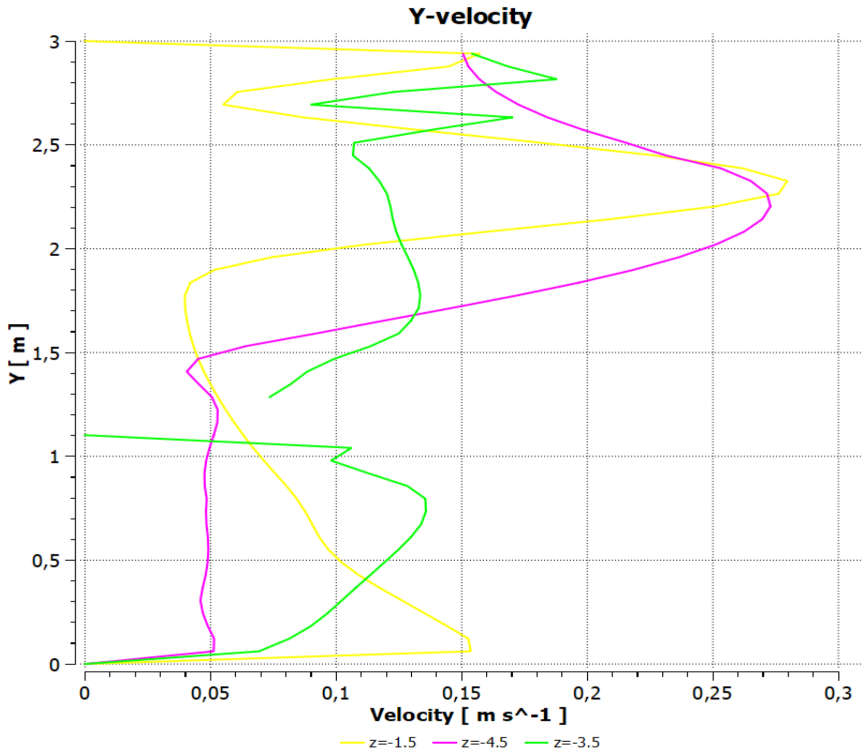

- The operating theatre and **big surgical lamp**: influence of dimensions lamp and position on velocity field
- The chart of velocity extract on the three lines (z=-1.5 yellow line, z=-3.5 green line, and z=-4.5 pink line)

Complete model: lamps position and size effects (2/2)

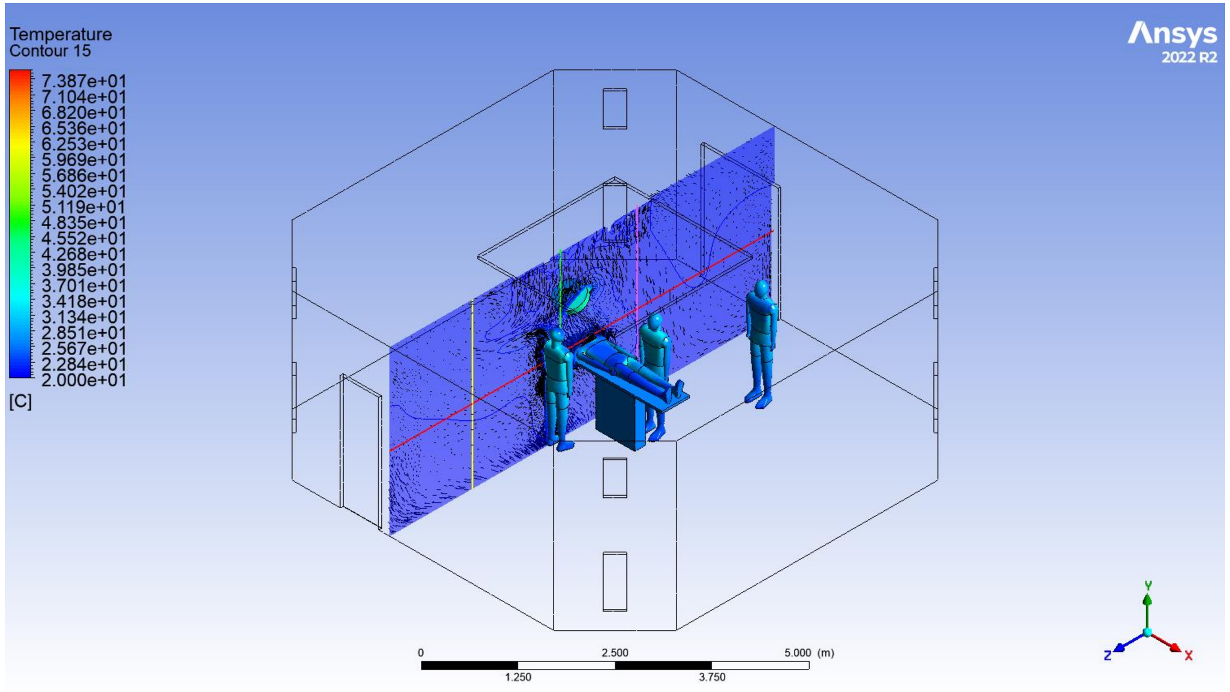

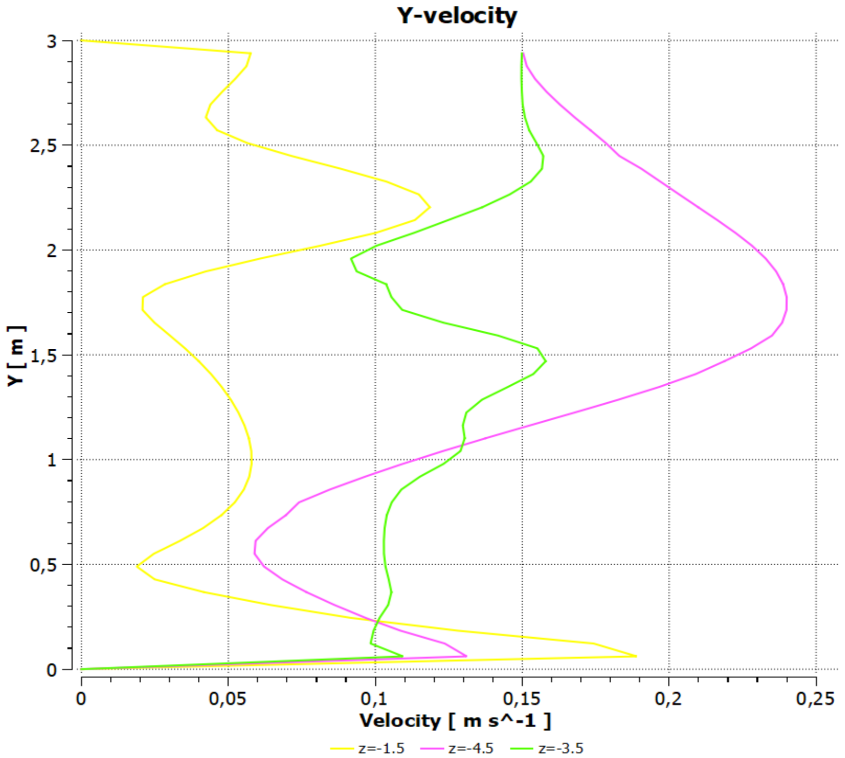

- The operating theatre and **small surgical lamp**: influence of dimensions lamp and position on velocity field
- The chart of velocity extract on the three lines (z=-1.5 yellow line, z=-3.5 green line, and z=-4.5 pink line)

Complete model: different system ventilations

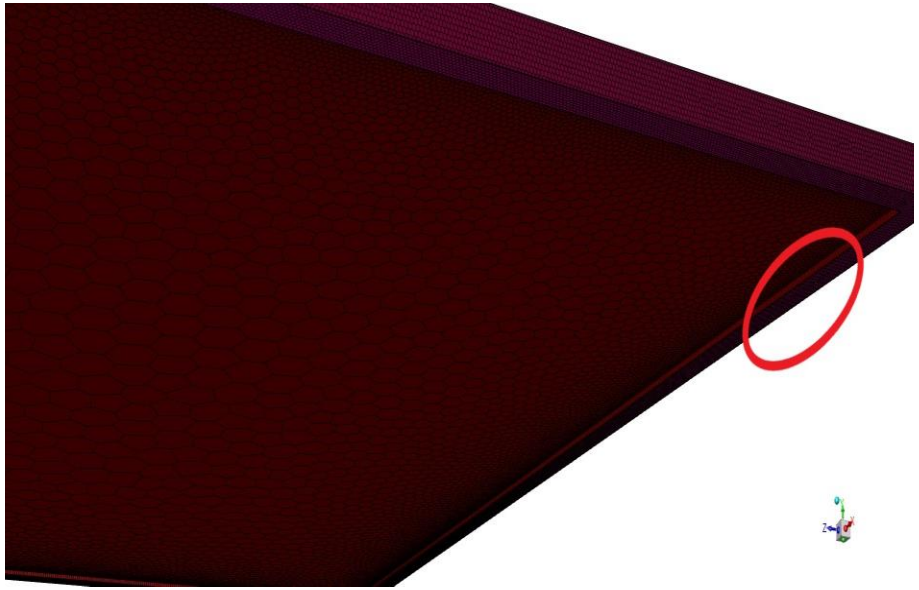

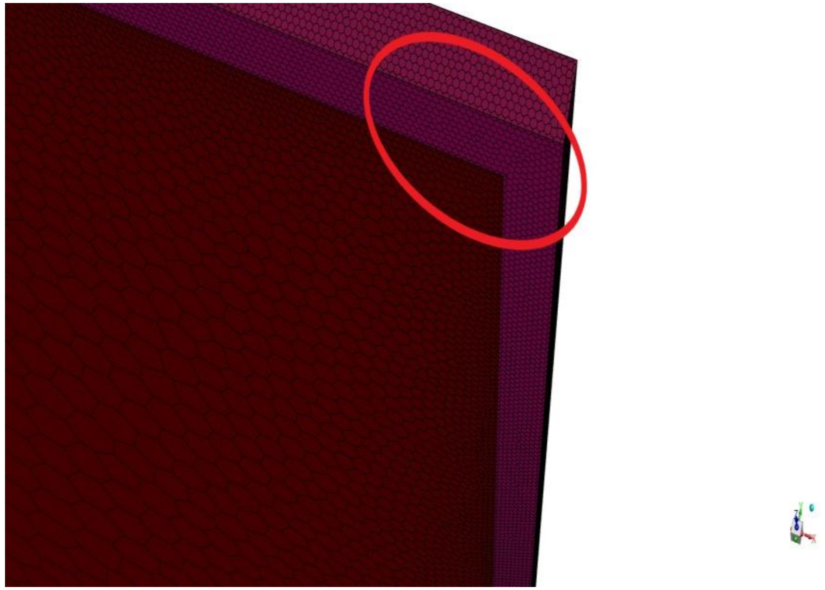

The different geometries for the ventilation systems ⇨ different kinds of air fluxes

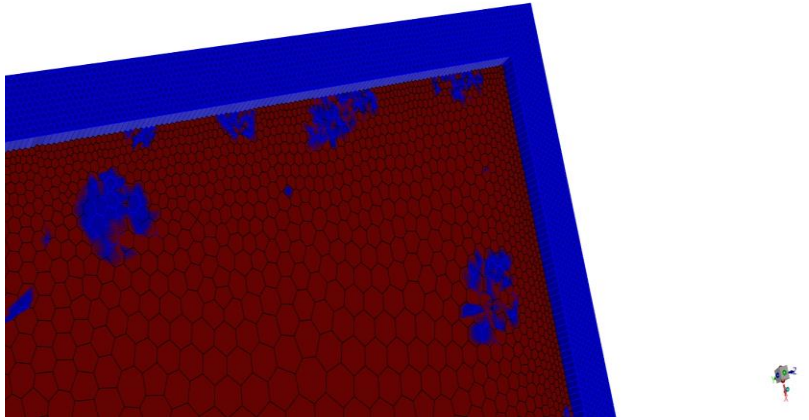

Conclusions

- **Archived results:**
- **Stationary simulations** with an operating room with a human dummy inside and **application of a power on the dummy** from which to evaluate the body temperature
- **Use of mixture** for the calculation of the relative humidity and to evaluate the CO_2 emitted during breathing
- **Comparison of CFD results and ROM results**: good approximation of ROM and digital twin over temperature and relative humidity range
- **The ROM responds in real-time** to the variation of the values of the variables: instantaneous evaluation of the quantities of interest
- The result of the ROM was exported to the **Twin Builder** software to obtain a **digital twin**
- **Preliminary study** to realize the experimental part

- **Further developments:**
- **complete** an operating theatre
- Possibility to **change simply the geometry** of operating theatre
- **experiments** on the mock-up

- **Critical analysis points:**
- **Further investigations** on the optimal number of samples to build the ROM

Thanks for your attention

Static ROM Builder

Working Directory: ...ers/giovg/Desktop/Papers_AIAA/articolo/temperature | 64 Snapshots - 8 Parameters | Browse | Set Geometry ROM | Help | Quit

Check | Input Reduction | Build | Validate | Evaluate

Field : Output Field **Display :** Average value over all field values (K)

Id	velocity_in_hvac	h2o_vap_in	move_input_param	co2_mouth	co2_in	pressure_out_grille	temperature_hvac
1	0.134	0.014	-0.734	4.972e-05	0.754	5.984	302.877
2	0.347	0.016	0.047	4.286e-05	0.796	6.734	291.595
3	0.491	0.027	0.109	3.599e-05	0.234	6.359	297.533
4	0.328	0.031	-0.453	6.573e-05	0.459	6.641	300.205
5	0.122	0.021	0.266	4.362e-05	0.909	3.172	293.377
6	0.466	0.025	0.078	6.421e-05	0.360	4.953	299.611
7	0.266	0.021	0.547	2.456e-05	0.374	2.609	293.673
8	0.497	0.014	-0.484	3.371e-05	0.529	5.891	308.814
9	0.166	0.022	0.734	3.828e-05	0.613	7.672	308.220
10	0.184	0.016	-0.578	2.913e-05	0.430	2.422	307.033
11	0.372	0.030	-0.266	2.227e-05	0.895	5.234	296.939
12	0.147	0.011	0.578	2.532e-05	0.726	4.391	302.283
13	0.391	0.024	-0.516	5.353e-05	0.149	2.797	307.923
14	0.334	0.013	0.297	6.344e-05	0.838	3.453	293.080
15	0.128	0.020	-0.766	6.192e-05	0.684	6.453	294.861
16	0.259	0.012	-0.953	2.989e-05	0.810	4.297	295.752
17	0.434	0.028	0.328	4.896e-05	0.698	5.422	309.705
18	0.309	0.029	0.984	5.582e-05	0.782	6.172	296.642
19	0.241	0.025	-0.859	3.066e-05	0.262	5.328	292.189
20	0.216	0.023	0.172	5.887e-05	0.641	3.359	310.002
21	0.303	0.011	-0.203	5.124e-05	0.866	3.078	307.330
22	0.416	0.011	-0.328	5.506e-05	0.388	7.766	296.048
23	0.422	0.021	0.672	4.667e-05	0.163	7.391	306.736
24	0.222	0.016	-0.359	2.151e-05	0.177	7.109	303.470
25	0.203	0.013	-0.297	3.752e-05	0.304	4.672	291.892
26	0.228	0.015	0.891	4.209e-05	0.135	3.734	303.173
27	0.428	0.019	0.828	2.761e-05	0.445	6.266	292.486
28	0.278	0.028	-0.984	3.294e-05	0.571	5.703	309.111
29	0.459	0.012	0.016	2.837e-05	0.276	2.984	298.423
30	0.172	0.026	0.422	2.608e-05	0.515	7.578	297.236
31	0.384	0.020	-0.391	2.074e-05	0.543	3.828	305.548

Points Size: 0.00 | Views : | FullModel | Parts | all

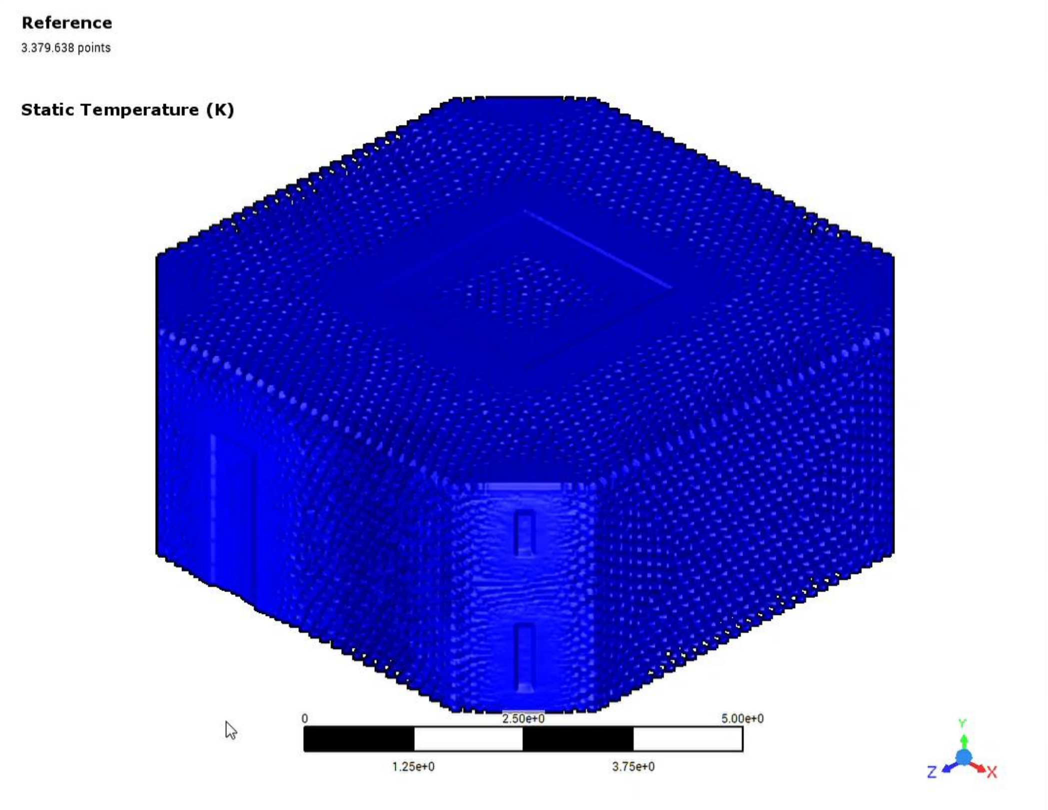

Project Read Ok.

Twin Builder

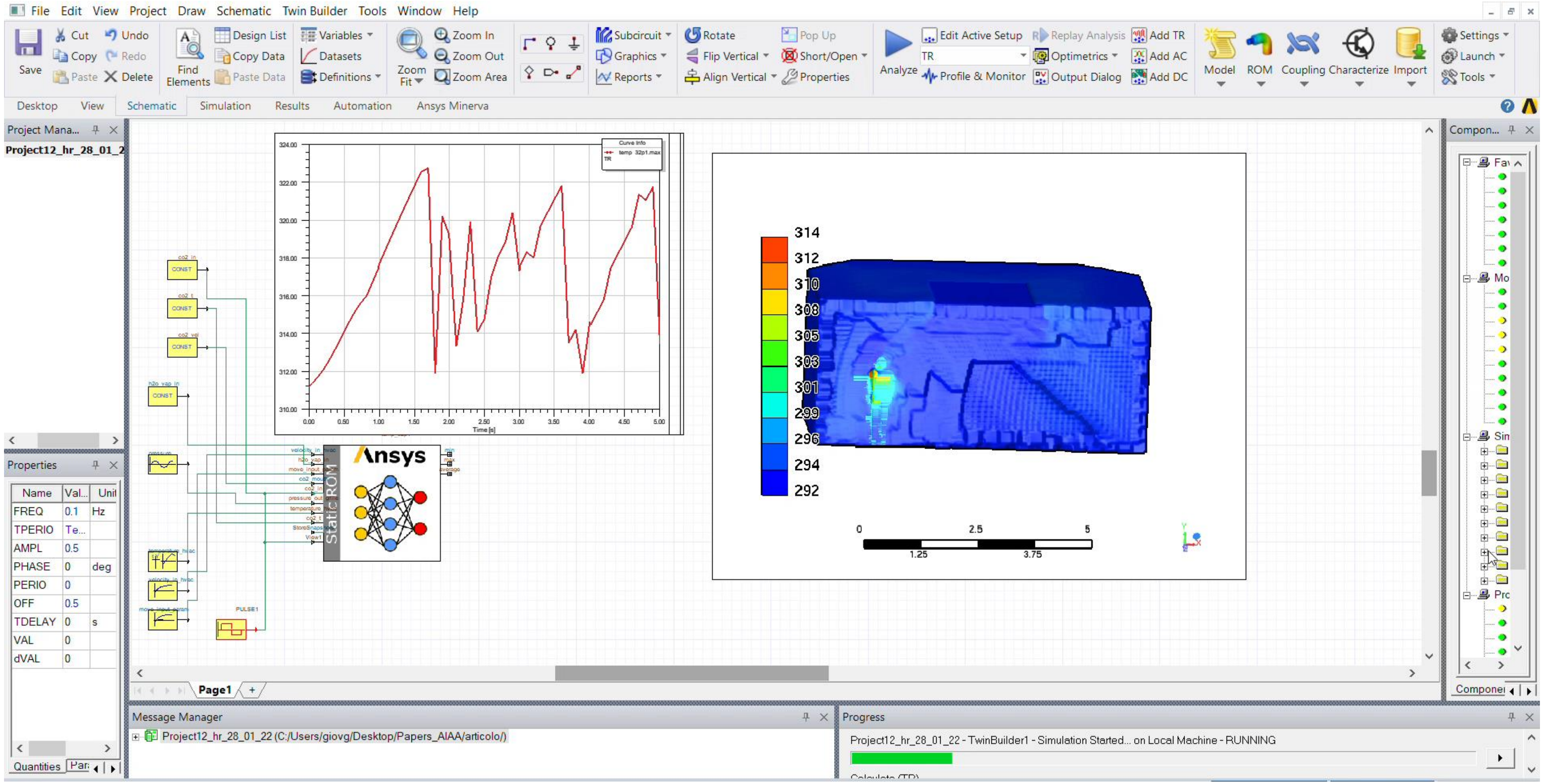

References (1/7)

[1] UNE *100713*:*2005*:Instalaciones de acondicionamiento de aire en hospitales - Air conditioning in hospitals, 2005.
[2] Partiicle Image Velocimetry. Cambridge University Press, 2011.
[3] Herve Abdi. Singular value decomposition (svd) and generalized singular value decomposition. Encyclopedia of measurement and statistics, 907:912, 2007. (pag 7).
[4] Amar Aganovic, Guangyu Cao, Liv-Inger Stenstad, and Jan Gunnar Skogas. Impact of surgical lights on the velocity distribution and airborne contamination level in an operating room with laminar airflow system. Building and Environment, 126:42–53, 2017.
[5] A Agodi, F Auxilia, M Barchitta, ML Cristina, D D'Alessandro, I Mura, M Nobile, C Pasquarella, Sergio Avondo, Patrizia Bellocchi, et al. Operating theatre ventilation systems and microbial air contamination in total joint replacement surgery: results of the gisio-ischia study. Journal of Hospital Infection, 90(3):213–219, 2015.
[6] Rafat Al-Waked. Effect of ventilation strategies on infection control inside operating theatres. Engineering Applications of Computational Fluid Mechanics, 4(1):1–16, 2010.
[7] Malin Alsved, Anette Civilis, Peter Ekolind, Ann Tammelin, A Erichsen Andersson, J Jakobsson, T Svensson, M Ramstorp, Sasan Sadrizadeh, PA Larsson, et al. Temperature-controlled airflow ventilation in operating rooms compared with laminar airflow and turbulent mixed airflow. Journal of Hospital Infection, 98(2):181–190, 2018.
[8] Inc ANSYS. Fluent User Guide. ANSYS, Inc, South Pointe 2600 Ansys Drive,Canonsburg, PA, USA., 2021. (pag 22 and 26).
[9] Inc ANSYS. Twin Builder Help risorse online. ANSYS, Inc, South Pointe 2600 Ansys Drive, Canonsburg, PA, USA., 2021.
[10] Inc ANSYS. Workbench Help risorse online. ANSYS, Inc, South Pointe 2600 Ansys
[11] LUCIO TIZIANO ARANEO, FEDERICO PEDRANZINI, LUIGI PIETRO COLOMBO, et al. Development of a scaled model for the experimental study of air flow patterns in a conditioned indoor space. In Proceedings of ASME-ATI-UIT *2015* Conference on Thermal Energy Systems: Production, Storage, Utilization and the Environment, pages 1–7, 2015.
[12] ANSI ASHRAE. Standard 170-2013. ventilation of health care facilities. American Society of Heating, Refrigerating and Air-Conditioning Engineers, Inc, Atlanta, 2013.
[13] Ashrae Handbook Fundamentals Ashrae and Ga Atlanta. American society of heating. Refrigerating and Air-Conditioning Engineers, 1, 2009.
[14] A Balducci, M Grigioni, Giorgio Querzoli, GP Romano, C Daniele, G D'Avenio, and V Barbaro. Investigation of the flow field downstream of an artificial heart valve by means of piv and ptv. Experiments in fluids, 36:204–213, 2004.
[15] Carla Balocco, Giuseppe Petrone, Giuliano Cammarata, et al. Numerical investigation of different airflow schemes in a real operating theatre. Journal of Biomedical Science and Engineering, 8(02):73, 2015.
[16] Carla Balocco, Giuseppe Petrone, Giuliano Cammarata, Pietro Vitali, Roberto Albertini, and Cesira Pasquarella. Indoor air quality in a real operating theatre under effective use conditions. Journal of Biomedical Science and Engineering, 2014, 2014.
[17] Malek Ben Salem, Olivier Roustant, Fabrice Gamboa, and Lionel Tomaso. Universal prediction distribution for surrogate models. SIAM/ASA Journal on Uncertainty Quantification, 5(1):1086–1109, 2017.

References (2/7)

[18] Malek Ben Salem and Lionel Tomaso. Automatic selection for general surrogate models. Structural and Multidisciplinary Optimization, 58(2):719–734, 2018.
[19] Sandra I Berrios-Torres, Craig A Umscheid, DaleWBratzler, Brian Leas, Erin C Stone, Rachel R Kelz, Caroline E Reinke, Sherry Morgan, Joseph S Solomkin, John E Mazuski, et al. Centers for disease control and prevention guideline for the prevention of surgical site infection, 2017. JAMA surgery, 152(8):784–791, 2017.
[20] Marco Evangelos Biancolini. Fast radial basis functions for engineering applications. Springer, 2017.
[21] M.E Biancolini. RBF for Fluent, User guide, 2021.
[22] Gabriel Birgand, Gaelle Toupet, Stephane Rukly, Gilles Antoniotti, Marie-Noelle Deschamps, Didier Lepelletier, Carole Pornet, Jean Baptiste Stern, Yves-Marie Vandamme, Nathalie van der Mee-Marquet, et al. Air contamination for predicting wound contamination in clean surgery: a large multicenter study. American journal of infection control, 43(5):516–521, 2015.
[23] Fernando Martin Biscione. Rates of surgical site infection as a performance measure: are we ready? World Journal of Gastrointestinal Surgery, 1(1):11, 2009.
[24] S. L Boer. A cfd study of operation room air conditioning: Air curtain performance. Master's thesis, Grand Valley State University, 12 2020.
[25] Spencer Lee Boer. A cfd study of operation room air conditioning: Air curtain performance. 2020.
[26] Osama Butt, Haider Latif, K Reinartz, G Hultmark, and A Afshari. Advanced airflow distribuition system for reducing airborne virus exposure in hospital rooms. In Indoor Air *2022*. ISIAQ, 2022.
[27] Guangyu Cao, Anders M Nilssen, Zhu Cheng, Liv-Inger Stenstad, Andreas Radtke, and Jan Gunnar Skogas. Laminar airflow and mixing ventilation: Which is better for operating room airflow distribution near an orthopedic surgical patient? American journal of infection control, 47(7):737–743, 2019.
[28] Zhu Cheng, Cao Guangyu, Amar Aganovic, and Li Baizhan. Experimental study of the interaction between thermal plumes and human breathing in an undisturbed indoor environment. Energy and Buildings, 207:109587, 2020.
[29] European Committee. EU-GMP - Guide to Good Manufacturing Practice, Annex *1*, Manufacture of Sterile Medicinal Products, 2008.
[30] Giuseppe D'Avenio, Mauro Grigioni, Carla Daniele, Umberto Morbiducci, and Kathrin Hamilton. 3d velocity field characterization of prosthetic heart valve with two different valve testers by means of stereo-piv. In *2015 37*th Annual International Conference of the IEEE Engineering in Medicine and Biology Society (EMBC), pages 3327–3330. IEEE, 2015.
[31] C Di Santis. Design and optimization of operating theater ventilation and contamination control system through an experimentally validated cfd model. Master's thesis, Politecnico di Milano, 2013.

References (3/7)

[32] Ente Nazionale Italiano di Unificazione. UNI EN ISO *14698*:*1- 2*, Camere bianche ed ambienti associati controllati: Controllo della biocontaminazione, 2004.

[33] Ente Nazionale Italiano di Unificazione. UNI EN *1822*:*2010* – parts *1-4*, Filtri per l'aria ad alta efficienza (EPA, HEPA e ULPA), 2010.

[34] Ente Nazionale Italiano di Unificazione. UNI *11425*:*2011*, Impianto di ventilazione e condizionamento a contaminazione controllata (VCCC) per il blocco operatorio - Progettazione, installazione, messa in marcia, qualifica, gestione e manutenzione, 2011.

[35] Ente Nazionale Italiano di Unificazione. UNI EN ISO *14644* – parts *1-10*, Cleanrooms and associated controlled environments, 2011.

[36] Ente Nazionale Italiano di Unificazione. UNI EN *779*:*2012*, Filtri d'aria antipolvere per ventilazione generale. Determinazione della prestazione di filtrazione, 2012.

[37] DDBE Du Bois. A formula to estimate the approximate surface area if height and weight be known. Nutrition, 5:303–313, 1989.

[38] PE Farhad Memarzadeh and Andrew P Manning. Comparison of operating room ventilation systems in the protection of the surgical site.

[39] FDA-Food. FDA-Food and Drag Administration-Current Good Manufacturing Practice, European Draft Guidance, 2008.

[40] D Ferrara. Experimental investigation of spray flow field and its interaction with uav wake. Master's thesis, Universita degli Studi di Napoli Federico II, 2022.

[41] Elizabeth U Finlayson, Ashok J Gadgil, Tracy L Thatcher, and Richard G Sextro. Pollutant dispersion in a large indoor space: Part 2-computational fluid dynamics (cfd) predictions and comparison with a scale model experiment for isothermal flow. 2002.

[42] Alfonso Gonzalez Gonzalez, Justo Garcia-Sanz-Calcedo, and David Rodriguez Salgado. A quantitative analysis of final energy consumption in hospitals in spain. Sustainable Cities and Society, 36:169–175, 2018.

[43] M Grigioni, A Amodeo, C Daniele, G D'Avenio, R Formigari, and RM Di Donato. Particle image velocimetry analysis of the flow field in the total cavopulmonary connection. Artificial organs, 24(12):946–952, 2000.

[44] Shamila Haddad, PAUL Osmond, and STEVE King. Metabolic rate estimation in the calculation of the pmv for children. In *47*th International Conference of the Architectural Science Association, pages 241–250. The Architectural Science Association Australia, 2013.

[45] X He, S Karra, P Pakseresht, SV Apte, and S Elghobashi. Effect of heated-air blanket on the dispersion of squames in an operating room. International journal for numerical methods in biomedical engineering, 34(5):e2960, 2018.

[46] Eirini Kardampiki, Emanuele Vignali, Dorela Haxhiademi, Duccio Federici, Edoardo Ferrante, Stefano Porziani, Andrea Chiappa, Corrado Groth, Margherita Cioffi, Marco Evangelos Biancolini, et al. The hemodynamic effect of modified blalock–taussig shunt morphologies: A computational analysis based on reduced order modeling. Electronics, 11(13):1930, 2022.

[47] Kishor Khankari. Hospital operating room ventilation systems. ASHRAE Journal, 60(6):16–26, 2018.

[48] Sihwan Lee, Beungyong Park, and Takashi Kurabuchi. Numerical evaluation of influence of door opening on interzonal air exchange. Building and environment, 102:230–242, 2016.

References (4/7)

[49] OM Lidwell, EJ Lowbury, W Whyte, R Blowers, SJ Stanley, and D Lowe. Effect of ultraclean air in operating rooms on deep sepsis in the joint after total hip or knee replacement: a randomized study. Br Med J (Clin Res Ed), 285(6334):10–14, 1982.
[50] Chunhua Liu, Guang Zhou, and Hongyuan Li. Analysis of thermal environment in a hospital operating room. Procedia Engineering, 121:735–742, 2015.
[51] Taishun Liu, Zeqin Liu, Ge Li, and Zhenjun Zuo. Comparative study of numerical simulation of indoor thermal environment in the pattern of personalized ventilation and stratum ventilation. Procedia Engineering, 121:785–791, 2015.
[52] Zhijian Liu, Haiyang Liu, Rui Rong, and Guoqing Cao. Effect of a circulating nurse walking on airflow and bacteria-carrying particles in the operating room: An experimental and numerical study. Building and Environment, 186:107315, 2020.
[53] Zhijian Liu, Haiyang Liu, Hang Yin, Rui Rong, Guoqing Cao, and Qihong Deng. Prevention of surgical site infection under different ventilation systems in operating room environment. Frontiers of Environmental Science & Engineering, 15(3):1–14, 2021.
[54] Gearoid P Lydon, Derek B Ingham, and Monjur M Mourshed. Ultra clean ventilation system performance relating to airborne infections in operating theatres using cfd modelling. In Building Simulation, volume 7, pages 277–287. Springer, 2014.
[55] Nicola Massarotti, Alessandro Mauro, Salahudeen Mohamed, Andrzej J Nowak, and Domenico Sainas. Fluid dynamic and thermal comfort analysis in an actual operating room with unidirectional airflow system. In Building Simulation, volume 14, pages 1127–1146. Springer, 2021.
[56] Sagnik Mazumdar, Stephane B Poussou, Chao-Hsin Lin, Sastry S Isukapalli, Michael W Plesniak, and Qingyan Chen. Impact of scaling and body movement on contaminant transport in airliner cabins. Atmospheric Environment, 45(33):6019–6028, 2011.
[57] James McNeill, Jean Hertzberg, and Zhiqiang John Zhai. Experimental investigation of operating room air distribution in a full-scale laboratory chamber using particle image velocimetry and flow visualization. 2013.
[58] James S McNeill, Zhiqiang John Zhai, and Jean Hertzberg. Field measurements of thermal conditions during surgical procedures for the development of cfd boundary conditions. ASHRAE Transactions, 118(2), 2012.
[59] Farhad Memarzadeh and Zheng Jiang. Effect of operation room geometry and ventilation system parameter variations on the protection of the surgical site. In Proceeding of IAQ, 2004.
[60] K Nowak, K Nowak-Dzieszko, and A Marcinowski. Analysis of ventilation air exchange rate and indoor air quality in the office room using metabolically generated co2. In IOP Conference Series: Materials Science and Engineering, volume 415, page 012028. IOP Publishing, 2018.
[61] C Pasquarella, M Barchitta, D D'Alessandro, ML Cristina, I Mura, M Nobile, F Auxilia, and A Agodi. Heating, ventilation and air conditioning (hvac) system, microbial air contamination and surgical site infection in hip and knee arthroplasties: The gisio-siti ischia study. 2018.

References (5/7)

[62] C Pasquarella, GE Sansebastiano, S Ferretti, E Saccani, M Fanti, U Moscato, G Giannetti, S Fornia, P Cortellini, P Vitali, et al. A mobile laminar airflow unit to reduce air bacterial contamination at surgical area in a conventionally ventilated operating theatre. Journal of Hospital Infection, 66(4):313–319, 2007.

[63] C Pasquarella, P Vitali, E Saccani, P Manotti, C Boccuni, M Ugolotti, C Signorelli, F Mariotti, GE Sansebastiano, and R Albertini. Microbial air monitoring in operating theatres: experience at the university hospital of parma. Journal of Hospital Infection, 81(1):50–57, 2012.

[64] Cesira Pasquarella, Antonella Agodi, Francesco Auxilia, Birgitta Lytsy, Ida Mura, Pierre Parneix, Walter Popp, and Silvio Brusaferro. Air quality in the operating theatre: a perspective. Aerobiologia, 36(1):113–117, 2020.

[65] Cesira Pasquarella, Carla Balocco, Maria Eugenia Colucci, Elisa Saccani, Samuel Paroni, Lara Albertini, Pietro Vitali, and Roberto Albertini. The influence of surgical staff behavior on air quality in a conventionally ventilated operating theatre during a simulated arthroplasty: a case study at the university hospital of parma. International journal of environmental research and public health, 17(2):452, 2020.

[66] Yang Peng, Ming Zhang, Fangqiang Yu, Jinglin Xu, and Shang Gao. Digital twin hospital buildings: an exemplary case study through continuous lifecycle integration. Advances in Civil Engineering, 2020.

[67] Istituto Superiore per la Prevenzione E la Sicurezza del Lavoro. ISPESL - Linee guida sugli standard di sicurezza e di igene del lavoro nel reparto operatorio, 2009.

[68] Marcelo Pereira, Arlindo Tribess, Giorgio Buonanno, Luca Stabile, Mauro Scungio, and Ilaria Baffo. Particle and carbon dioxide concentration levels in a surgical room conditioned with a window/wall air-conditioning system. International journal of environmental research and public health, 17(4):1180, 2020.

[69] Philip, Abouelmagd Maxemos, Hatem Abdelsamie, and Sadek. Review performance analysis of the ventilation system for the hospital operating room. American Journal of Engineering Research, 10(02):135–139, 2021.

[70] Stephane B Poussou, Sagnik Mazumdar, Michael W Plesniak, Paul E Sojka, and Qingyan Chen. Flow and contaminant transport in an airliner cabin induced by a moving body: Model experiments and cfd predictions. Atmospheric Environment, 44(24):2830–2839, 2010.

[71] Markus Raffel, Christian J. Kahler, Christian E. Willert, Steven T. Wereley, Fulvio Scarano, and Jurgen Kompenhans. Particle Image Velocimetry: A Practical Guide. Springer Science+Business Media, 3rd edition, 2018.

[72] Adil Rasheed, Omer San, and Trond Kvamsdal. Digital twin: Values, challenges and enablers from a modeling perspective. Ieee Access, 8:21980–22012, 2020.

[73] Francesco Romano, Luca Marocco, Jan Gusten, and Cesare M Joppolo. Numerical and experimental analysis of airborne particles control in an operating theater. Building and Environment, 89:369–379, 2015.

[74] Francesco Romano, Samanta Milani, Roberto Ricci, and Cesare Maria Joppolo. Operating theatre ventilation systems and their performance in contamination control:"at rest" and "in operation" particle and microbial measurements made in an Italian large and multi-year inspection campaign. International Journal of Environmental Research and Public Health, 17(19):7275, 2020.

References (6/7)

[75] Parastoo Sadeghian, Cong Wang, Christophe Duwig, and Sasan Sadrizadeh. Impact of surgical lamp design on the risk of surgical site infections in operating rooms with mixing and unidirectional airflow ventilation: A numerical study. Journal of Building Engineering, 31:101423, 2020.
[76] Sasan Sadrizadeh. Design of Hospital Operating Room Ventilation using Computational Fluid Dynamics. PhD thesis, KTH Royal Institute of Technology, 2016
[77] Sasan Sadrizadeh, Amar Aganovic, Anna Bogdan, Cong Wang, Alireza Afshari, Anne Hartmann, Cristiana Croitoru, Amirul Khan, Martin Kriegel, Merethe Lind, et al. A systematic review of operating room ventilation. Journal of Building Engineering, 40:102693, 2021.
[78] Sasan Sadrizadeh and Sture Holmberg. Effect of a portable ultraclean exponential airflow unit on the particle distribution in an operating room. Particuology, 18:170–178, 2015.
[79] Gonzalo Sanchez-Barroso and Justo Garcia Sanz-Calcedo. Evaluation of hvac design parameters in high-performance hospital operating theatres. Sustainability, 11(5):1493, 2019
[80] Eric B Smith, Ibrahim J Raphael, Mitchell G Maltenfort, Sittisak Honsawek, Kyle Dolan, and Elizabeth A Younkins. The effect of laminar air flow and door openings on operating room contamination. The Journal of arthroplasty, 28(9):1482–1485, 2013.
[81] JulianWTang, Andre Nicolle, Jovan Pantelic, Christian A Klettner, Ruikun Su, Petri Kalliomaki, Pekka Saarinen, Hannu Koskela, Kari Reijula, Panu Mustakallio, et al. Different types of dooropening motions as contributing factors to containment failures in hospital isolation rooms. PloS one, 8(6):e66663, 2013.
[82] Fei Tao, Bin Xiao, Qinglin Qi, Jiangfeng Cheng, and Ping Ji. Digital twin modeling. Journal of Manufacturing Systems, 64:372– 389, 2022.
[83] TL Thatcher, DJ Wilson, EE Wood, MJ Craig, and RG Sextro. Pollutant dispersion in a large indoor space: Part 1–scaled experiments using a water-filled model with occupants and furniture. Indoor Air, 14(4):258–271, 2004.
[84] Wei Tian, Thomas Alonso Sevilla, Wangda Zuo, and Michael D Sohn. Coupling fast fluid dynamics and multizone airflow models in modelica buildings library to simulate the dynamics of hvac systems. Building and Environment, 122:269–286, 2017.
[85] Albertus Anuello Louis Roberto Traversari. Aerogenic contamination control in operating theatres: studies towards effective use of udf systems. 2019.
[86] W Uyttenhove, M De Paepe, and A Janssens. Cfd-modelling of temperature and humidity distribution in the st. pieter's church. IAE-Annex *41*, Subtask, 1, 2004.
[87] Eric VanDerHorn and Sankaran Mahadevan. Digital twin: Generalization, characterization and implementation. Decision Support Systems, 145:113524, 2021.
[88] JM Villafruela, Ines Olmedo, M Ruiz De Adana, C Mendez, and Peter V Nielsen. Cfd analysis of the human exhalation flow using different boundary conditions and ventilation strategies. Building and Environment, 62:191–200, 2013.
[89] Fujen Wang, Indra Permana, Dibakar Rakshit, and Bowo Yuli Prasetyo. Investigation of airflow distribution and contamination control with different schemes in an operating room. Atmosphere, 12(12):1639, 2021

References (7/7)

[90] Julien Weiss. A tutorial on the proper orthogonal decomposition. In AIAA Aviation *2019* Forum, page 3333, 2019.
[91] William Whyte, D Vesley, and R Hodgson. Bacterial dispersion in relation to operating room clothing. Epidemiology & Infection, 76(3):367–378, 1976.
[92] Yan-Lin Wu, Yu-Lieh Wu, and Azka Hasya Hanifan. Study on ventilation performance in operating room with variation ventilation design. In Journal of Physics: Conference Series, volume 1500, page 012040. IOP Publishing, 2020.
[93] Chao-Tung Yang, Chi-Jui Liao, Jung-Chun Liu, Walter Den, Ying- Chyi Chou, and Jaw-Ji Tsai. Construction and application of an intelligent air quality monitoring system for healthcare environment. Journal of medical systems, 38(2):1–10, 2014.
[94] Zhiqiang John Zhai and Anna L Osborne. Simulation-based feasibility study of improved air conditioning systems for hospital operating room. Frontiers of Architectural Research, 2(4):468–475, 2013.
[95] Bin Zhou, Lili Ding, Fei Li, Ke Xue, Peter V Nielsen, and Yang Xu. Influence of opening and closing process of sliding door on interface airflow characteristic in operating room. Building and Environment, 144:459–473, 2018.
[96] Wangda Zuo, Michael Wetter, Wei Tian, Dan Li, Mingang Jin, and Qingyan Chen. Coupling indoor airflow, hvac, control and building envelope heat transfer in the modelica buildings library. Journal of Building Performance Simulation, 9(4):366–381, 2016
[97] Zhenjun Zuo. Buildings Examples Tutorial Boiler https://simulationresearch.lbl.gov/modelica/releases/v5.0.0/help/Buildings_Examples_Tutorial_Boiler.html, 2021. [Online; accessed June 08, 2021].

Publications

Papers

- A Digital Twin of an Operating Theatre - G. Gargiulo, C.Groth, M.E. Biancolini, M. Grigioni, G. D'Avenio - 18th Healthy Buildings Europe Conference, 11th – 14th June 2023, Aachen, Germany
- Gemello Digitale di una Sala Operatoria - G. Gargiulo, C.Groth, M.E. Biancolini, M. Grigioni, G. D'Avenio - Analisi e Calcolo n.ro 107, pagine 8-13. Link https://aec-analisiecalcolo.it/pubblicazioni/aec/107/gemello-digitale-di-una-sala-operatoria
- Emergenza COVID-19: studio del sistema dei ricoveri e delle risposte nei modelli organizzativi nelle diverse regioni italiane. - Simona Anelli, Chiara Baratta, Emilia Barberini, Giovanna Gargiulo, Sara Lucarini, Fabrizio Pecoraro, Fabrizio Clemente - Smart eLab, volume 15, anno 2020. Link https://calliope.cnr.it/index.php/smartelab/article/view/170

Presentation

- Poster session in Summer School on ROMs in CFD - SISSA (Scuola Internazionale Superiore di Studi Avanzati), 13/07-2022.
- The result of the combination of Twin Builder + RBF Morph per Fluent 2021 R1 (2021)
- The building of the ROM during the Ottimizzazione multi fisica nell'industria aeronautica (2021)

Influence factors: further details

- Ventilation systems
- Number of opening doors

Ventilation Systems

	Airflow distribuited concept	Location of supply	Location of exhaust	Air supply conditions - studies		
				Velocity (m/s)	Air Change per Hour (ACH)	Diffuser size (m^2)
Turbulent Flow Air Distribution (TFAD)	The concentration of airborne contaminants is diluted by mixing the supply air with the contaminated OR air	Ceiling or wall - mounted	Wall mounted near floor	-	11.5–23.; 15.5–21.3; 50	-
Vertical Laminar Airfow (vLAF)	The unidirectional airflow swipes away the contaminants over the operating microenvironment	Ceiling - mounted	Ceiling and/or wall mounted near floor	0.25–0.38	5.3–27.6; 26-178; 80.5; 58; 15.1–59.9; 67; 100	2.4 × 2.4–3.2 × 3.2; 3.8 × 1.2–5.18 × 3.83; 3.2 × 3.2; 3.6 × 3.6; 2.75 × 2.75
Horizontal Laminar Airflow (hLAF)		Wall -mounted	Ceiling and/or wall mounted near floor			
Mobile Laminar Airflow (mLAF)		Mobile: In the vicinity of the operating table -	Ceiling and/or wall mounted near floor	0.5–**0.7**	8.4	0.5 × 0.4; 0.69 × 0.7
Displacement Ventilation Airflow (DV)	Cool air is supplied at floor level and is moved up displacing the contaminated air from the operating microenvironment	Wall mounted near floor	Ceiling or wall mounted near ceiling	**0.09**–0.15	21	-
Temperature Controllated Airflow (TAF)	Combination of LAF (cool laminar airflow breaking convective currents in the operating microenvironment) and TFW (warm air maintaining temperature gradient)	Both cool and warm air is supplied from the ceiling	Wall mounted near floor	>0.25	47	-

Opening doors

Type of surgery	Ventilation type	Door opening frequency [Openings/h]	Monitoring contamination/SSI?	Association between door openings and contamination?	Association between door openings and SSI rate?
Abdominal	Mixing	59.3	SSI	-	Yes
Cardiac/ orthopaedic	LAF/Mixing	20.2	Particles/CFU	Yes/Yes	-
Orthopaedic	Unknown	27.0–34	-	-	-
Cardiac	LAF	32.4	SSI	-	Yes
orthopaedic	LAF/Mixing/ TcAF	2.1–5.6	CFU	No	-
Total joint arthroplasty	LAF	19.2–21.6	-	-	-
Orthopaedic/ general	LAF	12.6–36.6	CFU	Yes	-
Plastic surgery	Unknown	13.4	Particles	Yes	-
Neurosurgery	LAF	46.2	SSI	-	No
Hip revision	Mixing	3.3	CFU	Yes	-
Cardiac/general	Unknown	33–54	-	-	-
Joint Arthroplasty	Mixing	16.6–37.3	SSI	-	Unclear
Orthopaedic	LAF	37.2	CFU	Yes	-
Orthopaedic	Displacement	12.5	CFU	Yes	-
Colorectal	Unknown	-	SSI	-	Yes
Total joint arthroplasty	LAF	41.4	-	-	-
Cardiac	Unknown	19.2	SSI	-	Yes
Joint Arthroplasty	Mixing	33.6	Particles/CFU	-/No	-
Multiple	Unknown	19–50	-	-	-
Orthopaedic/ urology/general	Mixing	56.4	Particles/CFU	No/Yes	-

Curve reduction and LOO

- The curve **Reduction** represents the precision of the learning set with respect to the number of modes
- The curve **LOO (Leave One Out) define** the **precision of the base** of the modes for **a snapshot not included** in **the learning set**